ESA Climate Change Initiative “Plus” (CCI+)

Product Validation and Intercomparison Report (PVIR)

for the Essential Climate Variable (ECV)

Greenhouse Gases (GHG):

XCO_2 and/or XCH_4 from OCO-2, TanSat,

Sentinel-5-Precursor and GOSAT-2

Written by:

GHG-CCI+ project team

Lead author: Michael Buchwitz, Institute of Environmental Physics (IUP), University of Bremen, Germany

Co-authors:

Bart Dils (BIRA-IASB, Belgium, Brussels)

Maximilian Reuter, Oliver Schneising (IUP, Univ. Bremen, Germany)

Hartmut Boesch, Dongxu Yang (Univ. Leicester, UK)

Ilse Aben, Enrico Dammers (SRON, Utrecht, The Netherlands)

Change log:

Version Nr.	Date	Status	Reason for change
Version 1	17-Feb-2020	As submitted to ESA	New document
Version 1.1	13-Mar-2020	Final	Several (minor) improvements

Table of Contents

1 Executive Summary

This document is the Product Validation and Intercomparison Report (PVIR) version 1.1 (v1.1), which is a deliverable of the ESA project GHG-CCI+ (http://cci.esa.int/ghg). The GHG-CCI+ project, which started in March 2019, is carrying out the research and development (R&D) needed to generate new Greenhouse Gas (GHG) Essential Climate Variable (ECV) satellite-derived CO_2 and CH_4 data products. These products are column-averaged dry-air mole fractions of carbon dioxide (CO_2), denoted XCO_2, and methane (CH_4), denoted XCH_4, from these satellites / satellite sensors using European scientific retrieval algorithms:

- XCO_2 from OCO-2 using the University of Bremen FOCAL algorithm (product **CO2_OC2_FOCA**),
- XCH_4 from Sentinel-5 Precursor (S5P) using University of Bremen's WFM-DOAS (or WFMD) algorithm (product **CH4_S5P_WFMD**),
- XCO_2 from TanSat using University of Leicester UoL-FP (or OCFP) algorithm (product **CO2_TAN_OCFP**; global product in preparation; current product only at TCCON sites), and
- XCO_2 and XCH_4 from GOSAT-2 using SRON's RemoTeC algorithm (products **CO2_GO2_SRFP, CH4_GO2_SRFP, CH4_GO2_SRPR**; in preparation; first products will be released in March 2021)

This project aims to generate GHG ECV data products in-line with GCOS (Global Climate Observing System) requirements. GCOS defines the ECV GHG as follows: “Retrievals of greenhouse gases, such as CO_2 and CH_4, of sufficient quality to estimate regional sources and sinks”. Within the GHG-CCI+ project satellite-derived XCO_2 (in ppm) and XCH_4 (in ppb) data products are retrieved from satellite radiance observations in the Short-Wave-Infra-Red (SWIR) spectral region. These instruments are used because their measurements are sensitive also to the lowest atmospheric layer and therefore provide information on the regional surface sources and sinks of CO_2 and CH_4. All products are generated with independent retrieval algorithms developed to convert GOSAT-2, OCO-2, TanSat and/or TROPOMI/S5P radiance spectra into Level 2 (L2) XCO_2 and/or XCH_4 data products.

In this document initial validation and intercomparison results are presented. The validation is based on comparisons with TCCON (Total Carbon Column Observation Network) ground-based XCO_2 and XCH_4 retrievals. The validation has been carried out by the GHG-CCI+ independent Validation Team (VALT) and by the data provider (DP) of a given product. Note that the (initial GHG-CCI+ products) VALT assessments are based on a quite sparse data set (see Sect. 4 for details) and that it is planned to improve the VALT method for the next round of product validation. For each data product and each assessment method the following validation summary “figures of merit” have been determined and are reported in this document: (i) Single measurement precision, (ii) mean bias (global offset), (iii) relative systematic error (or relative accuracy), (iv) stability (linear bias drift or trend). Furthermore, also the reported XCO_2 and XCH_4 uncertainties have been validated by computing a quantity called “Uncertainty ratio”, which is the ratio of the (mean value of the) reported uncertainty and the standard deviation of satellite minus TCCON differences. The results are summarized in **Table 1** for the XCO_2 products and **Table 2** for the XCH_4 product.

Table 1: *Summary of the validation of XCO_2 products CO2_OC2_FOCA and CO2_TAN_OCFP of data set Climate Research Data Package No. 5 (CRDP#5, released in March 2020) via comparison with TCCON ground-based XCO_2 retrievals (using version GGG2014). VALT refers to the assessment results of the GHG-CCI+ independent validation team and DP refers to the assessment results of the data provider. (*) Excluding a possible global offset, which is reported separately in this document.*

Summary validation results GHG-CCI+ CRDP#5 XCO_2 products by comparisons with TCCON (GGG2014)			
Product CO2_OC2_FOCA (v08, global, 2015 – 2018)			
Parameter	**Achieved**	**Required**	**Comments**
Random error (single obs., 1σ) [ppm]	VALT: 1.94 DP: 1.52	T:<8; B:<3; G:<1	T=threshold; B=breakthrough; G=goal
Systematic error [ppm]	VALT: 0.73 / 0.96 DP: 0.64 / 0.74	< 0.5	"Relative accuracy" (*) Spatial / spatio-temp.
Stability: Linear bias trend [ppm/year]	VALT: -0.16 ± 0.06 DP: 0.00 ± 0.75	< 0.5	1σ uncertainty
Product CO2_TAN_OCFP (v1, 1 year @ TCCON)			
Parameter	**Achieved**	**Required**	**Comments**
Random error (single obs., 1σ) [ppm]	VALT: 2.33 DP: 1.78	T:<8; B:<3; G:<1	T=threshold; B=breakthrough; G=goal
Systematic error [ppm]	VALT: 0.93 / 1.75 DP: 0.84 / n.a.	< 0.5	"Relative accuracy" (*) Spatial / spatio-temp.
Stability: Linear bias trend [ppm/year]	VALT: 0.2 ± 0.6 DP: n.a.	< 0.5	1σ uncertainty Only short time period

Table 2: *Summary of the validation of XCH_4 products CH4_S5P_WFMD of data set Climate Research Data Package No. 5 (CRDP#5, released in March 2020) via comparison with TCCON ground-based XCH_4 retrievals (using version GGG2014). VALT refers to the assessment results of the GHG-CCI+ independent validation team and DP refers to the assessment results of the data provider. (*) Excluding a possible global offset, which is reported separately in this document.*

Summary validation results GHG-CCI+ CRDP#5 XCH_4 products by comparisons with TCCON (GGG2014)			
Product CH4_S5P_WFMD (v1.2, global, Nov.2017– Dec.2018)			
Parameter	**Achieved**	**Required**	**Comments**
Random error (single obs., 1σ) [ppb]	VALT: 20 DP: 14	T:<34; B:<17; G:<9	T=threshold; B=breakthrough; G=goal
Systematic error [ppb]	VALT: 6.5 / 8.8 DP: 4.3 / 4.4	< 10	"Relative accuracy" (*) Spatial / spatio-temp.
Stability: Linear bias trend [ppb/year]	VALT: 6.7 ± 4.3 DP: n.a.	< 3	1σ uncertainty Only short time period

2 Introduction

This document is the Product Validation and Intercomparison Report (PVIR) version 1.1 (v1.1), which is a deliverable of the ESA project GHG-CCI+ (http://cci.esa.int/ghg).

The GHG-CCI+ project, which started in March 2019, is carrying out the R&D needed to generate new Greenhouse Gas (GHG) Essential Climate Variable (ECV) satellite-derived CO_2 and CH_4 data products.

These products are column-averaged dry-air mole fractions of carbon dioxide (CO_2), denoted XCO_2, and methane (CH_4), denoted XCH_4, from these satellites / satellite sensors using European scientific retrieval algorithms:

- XCO_2 from OCO-2 and TANSAT,
- XCO_2 and XCH_4 from GOSAT-2 and
- XCH_4 from S5P

This project aims to generate GHG ECV data products in-line with GCOS (Global Climate Observing System) requirements **/GCOS-154/ /GCOS-195/ /GCOS-200/**. GCOS defines the ECV GHG as follows: "Retrievals of greenhouse gases, such as CO_2 and CH_4, of sufficient quality to estimate regional sources and sinks".

Once the products are of sufficient quality for a climate service and cover a long enough time period, it is expected that the data will become part of the Copernicus Climate Change Service (C3S, https://climate.copernicus.eu/).

Within GHG-CCI+ satellite-derived XCO_2 (in ppm) and XCH_4 (in ppb) data products are retrieved from satellite radiance observations in the Short-Wave-Infra-Red (SWIR) spectral region. These instruments are used because their measurements are sensitive also to the lowest atmospheric layer and therefore provide information on the regional surface sources and sinks of CO_2 and CH_4.

This document provides validation and intercomparison results for the XCO_2 and XCH_4 datasets as listed in **Table 3** for XCO_2 and **Table 4** for XCH_4.

All products are generated with independent retrieval algorithms developed to convert GOSAT-2, OCO-2, TANSAT and/or TROPOMI/S5P radiance spectra into Level 2 (L2) XCO_2 and/or XCH_4 data products.

For more information on these products see also **Table 5**.

Table 3: *Overview GHG-CCI+ algorithms for XCO_2 retrieval. # Currently only retrievals at TCCN sites are available. * First products will be available in the 2nd year of this project.*

XCO_2 Product Identifier	**Algorithm (version)**	**Institute**	**Technique**	**Reference**
CO2_OC2_FOCA	FOCAL (v08)	IUP, Univ. Bremen, Germany	Optimal Estimation; approximation for an optically thin Lambertian scattering layer	Reuter et al., 2017a, b
CO2_TAN_OCFP	UoL-FP (v1, #)	Univ. Leicester (UoL), United Kingdom	Optimal Estimation	Boesch et al., 2011
CO2_GO2_SRFP	SRFP or RemoTeC (*)	SRON, Netherlands	Phillips-Tikhonov regularization	Butz et al., 2009, 2010

Table 4: *Overview GHG-CCI+ algorithms for XCH_4 retrieval. * First products will be available in the 2nd year of this project.*

XCH_4 Product Identifier	**Algorithm (version)**	**Institute**	**Technique**	**Reference**
CH4_S5P_WFMD	WFM-DOAS (v1.2)	IUP, Univ. Bremen, Germany	Weighted least squares	Schneising et al., 2019
CH4_GO2_SRPR	SRPR or RemoTeC (*)	SRON, Netherlands	Proxy (PR) retrieval method	Frankenberg et al., 2005
CH4_GO2_SRFP	SRFP or RemoTeC (*)	SRON, Netherlands	Phillips-Tikhonov regularization; Full Physics (FP) method	Butz et al., 2009, 2010

Table 5: *Overview of (other) GHG-CCI+ product related documents. ATBD = Algorithm Theoretical Basis Document, PUG = Product User Guide, E3UB = End-to-End ECV Uncertainty Budget document.*

Product ID	Document	Link
CO2_OC2_FOCA	ATBD	http://cci.esa.int/sites/default/files/ATBDv1_OCO2_FOCAL.pdf
-"-	PUG	http://cci.esa.int/sites/default/files/PUGv2_GHG-CCI_CO2_OC2_FOCA_v08.pdf
-"-	E3UB	http://cci.esa.int/sites/default/files/E3UBv1_GHG-CCI_CO2_OC2_FOCA_v08.pdf
CH4_S5P_WFMD	ATBD	http://cci.esa.int/sites/default/files/ATBDv1_S5P_WFMD.pdf
-"-	PUG	http://cci.esa.int/sites/default/files/PUGv1_GHG-CCI_CH4_S5P_WFMD.pdf
-"-	E3UB	http://cci.esa.int/sites/default/files/E3UBv1_GHG-CCI_CH4_S5P_WFMD_v2.pdf
CO2_TAN_OCFP	ATBD	http://cci.esa.int/sites/default/files/ATBDv1_TanSat_CCIp_UoL.pdf
-"-	PUG	http://cci.esa.int/sites/default/files/PUGv1_GHG-CCI_CO2_Tan_OCFP_v1.1.pdf
-"-	E3UB	http://cci.esa.int/sites/default/files/E3UBv1_GHG-CCI_CO2_TAN_OCFP_v1.1.pdf

3 General description of the processing system

A schematic overview of the GHG-CCI+ processing system is given in **Figure 1**.

The processing system consists of the different algorithms (see **Table 3** and **Table 4**), running at the different responsible institutes.

The different institutes have their own access to the required input data (satellite data, ECMWF meteo data, model data for priors, spectroscopic databases, etc.), and their own computational facilities in the form of multi CPU Unix/Linux systems.

The Level-2 (L2) output data (XCO_2 and XCH_4) generated by the algorithms at the different institutes are available via the CCI Open Data Portal (http://cci.esa.int/data) and additional information is given at the GHG-CCI+ website (http://cci.esa.int/ghg).

The different parts of the GHG-CCI+ processing systems running at the different institutes are described in more detail in the System Specification Document (SSD) document **/Aben et al., 2019/**.

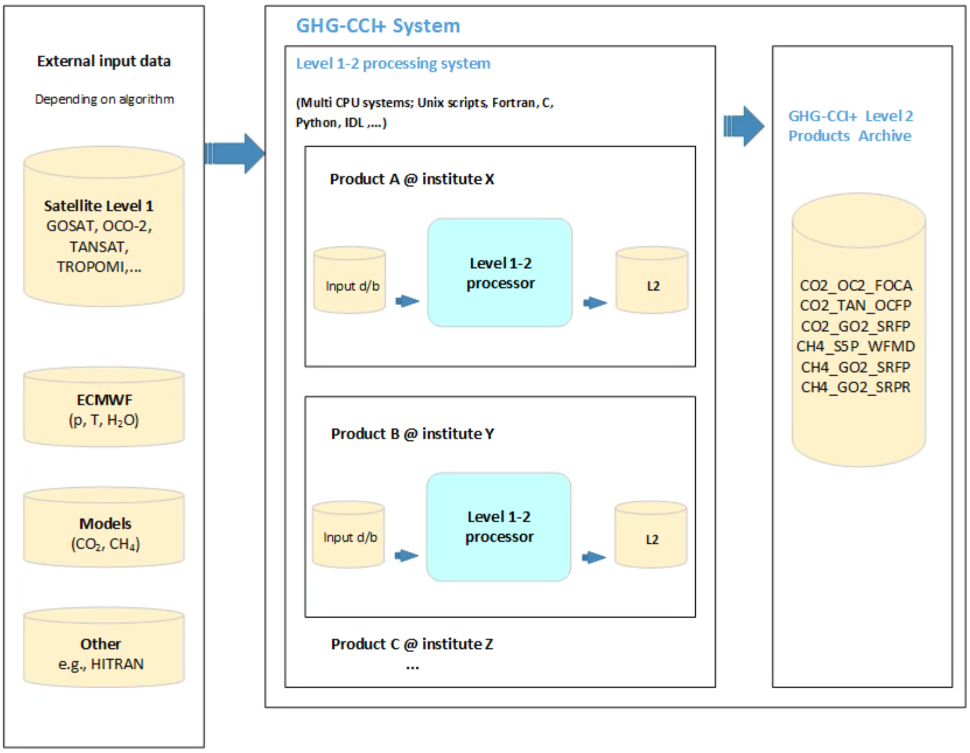

Figure 1: *Overview of the GHG-CCI+ processing system. Note that the GHG-CCI+ Level 2 product data archive is the CCI Open Data Portal (http://cci.esa.int/data).*

4 Independent validation by validation team

This chapter deals with the validation of the GHG-CCI+ retrieval products using ground-based FTIR remote sensing measurements from the Total Carbon Column Observing Network (TCCON) **/Wunch et al.2011/**. There are several key changes with regards to the methodology employed during the last stage of the predecessor GHG-CCI project (see **/PVIRv5, 2017**/ for details). Foremost, at this stage, no competing algorithms (sharing the same instrument and product) are present. This in effect greatly simplifies the methodology, as the statistical analysis of the differences between 2 competing algorithms is not present. Also removed is the replacement of the satellite apriori profiles with that of TCCON. This was essentially done to bring competing algorithms on the same playing field as far as the apriori was concerned. Given the nature of TCCON retrievals (post-corrected profile scaling), such a replacement would be of dubious benefit in the current context.

As always choosing collocation criteria is a balance between minimizing the potential collocation error and still retaining a large enough sample so as to be able to derive adequate statistics. Also of note is that the current available timeseries are rather short in the case of CO2_TAN_OCFP and CH4_S5P_WFMD. Only the CO2_OC2_FOCA dataset covers a more substantial 4 year period. As a result, the size of the dataset retained after collocation remains fairly small as we did not want to overextend the collocation criteria either. This entails that some parameters are very hard to correctly assess. With time and additional data we are confident that our analysis will become more robust.

Concerning the Figures of Merit (FoM), we did not employ any averaging and looked at individual satellite-TCCON pairs. This was done mainly to have statistical parameters that relate to the quality of the original data. Users of the data however should keep in mind that some algorithms opt to have a high density dataset with a larger random error component versus a much stricter quality-flagged low density dataset with a smaller random error component. After averaging (in space or time) the first might outperform the latter.

4.1 Validation method

Each individual TCCON measurement is paired, if the criteria are met, with an individual satellite measurement. This particular satellite measurement needs to be taken within 2 hours and within 250 km of the TCCON measurement. If more than one satellite measurement fits the above criteria, the satellite measurement that has been measured closest (in space) to the TCCON station will be the one paired with said TCCON measurement.

This creates a collocated dataset with unique satellite-TCCON pairs on which we perform our validation analysis and derive our so-called Figures of Merit (FoM). For certain plots and the overview table, we averaged the timeseries into daily averages. The bias is defined as the mean difference between satellite and TCCON pairs

$$\text{Bias}=\text{mean}(X_{sat}-X_{FTS}) \qquad (4.1)$$

While the scatter corresponds with the standard deviation of said difference as in:

$$\text{Scatter}=\text{std}(X_{sat}-X_{FTS}) \qquad (4.2)$$

Both parameters are presented with their 95% confidence interval in the validation summary tables (see **Table 5, Table 8, Table 11**).

Other FoM are the Relative accuracy (RA) and Seasonal Relative Accuracy (SRA), who give an indication of the spatial and spatio-temporal accuracy of the algorithm. We define RA as the standard deviation on the overall median biases (derived from individual data) obtained at each station. Note that, for the calculation of the RA and SRA, we took the median of the satellite and TCCON differences at each station, instead of the mean to reduce the potential impact of individual outliers. The "Seasonal Relative Accuracy" (SRA), differs from the relative accuracy in that it uses the seasonal bias medians at each station, instead of the overall biases obtained at each station, it is thus the standard deviation over all station seasonal median bias results. The seasonal bias results are constructed, for each TCCON station, from all data pairs which fall within the months of January till March (JFM), April till June (AMJ), July till September (JAS) or October till December (OND), regardless of the year the measurements are taken. Some stations feature only limited data during certain seasons, which sometimes results in erratic (seasonal) bias results. To avoid the inclusion of these results into the RA and SRA calculation, we do not include those results which are derived from less than 10 individual unique satellite measurements.

We have used all public TCCON GGG2014 data as available on the TCCON Data Archive (https://tccondata.org/) on the 1st of February 2020 in our initial analysis. For the determination of the statistical parameters we did remove several sites from the roster, foremost the high altitude sites Zugspitze and Izaña, while others were removed due to lack of data.

Another Figure of Merit is the so-called Uncertainty Ratio, which is defined as the ratio between the algorithm's reported uncertainty and the above mentioned scatter (standard deviation of satellite-TCCON difference). If the reported uncertainty is correctly assessed, the uncertainty ratio should approach unity. However, this baseline number ignores any aspect of temporal, spatial or TCCON variability embedded in the scatter.

We therefore also calculate an improved Uncertainty Ratio, which is the ratio between the reported uncertainty and the uncertainty on the Satellite (σ_{SAT}) as determined from the scatter using the method outlined below. Both are reported in the summary tables of each algorithm (see **Table 5, Table 8, Table 11**), where the improved uncertainty ratio is marked by an *.

Taking into account the variability of the TCCON reference data and the collocation error, when assuming independence, the scatter can be written down as:

$$\text{scatter}=\sqrt{(\sigma_{SAT}^2+\sigma_{TCCON}^2+\sigma_{Collocation}^2)} \qquad (4.3)$$

where σ_{SAT} is the standard deviation due to variability of the satellite product, σ_{TCCON} due to variability within TCCON and $\sigma_{Collocation}$ due to variability in time and space.
σ_{SAT} as derived from our comparison between the satellite and TCCON measurements is thus:

$$\sigma_{SAT}=\sqrt{(scatter^2-\sigma_{TCCON}^2-\sigma_{Collocation}^2)} \qquad (4.4)$$

The standard deviation on the TCCON measurements can be readily calculated from the average variability of the FTIR measurements within the collocation timeframe (4 hours) that match up with a single satellite measurement.

The Collocation uncertainty is harder to define and consists of a spatial and temporal component. The latter can be ignored since it is already embedded in our calculation of the TCCON uncertainty (which is based on the actual variability of the TCCON measurements in time and thus also contains the temporal natural variability).

Unfortunately we have no solid information on the spatial collocation uncertainty. Our best, but flawed, estimate of this factor can be derived from fitting the sat-TCCON residuals as a function of distance between the TCCON site and the satellite pixel center point. This yields a value for the deviation from the centre point given a certain distance. Ideally, to deterime the standard deviation we need to look at a distance from the centre that encapsulates 68% of the population. Given that we use a collocation method that is predicated on finding the closest (in distance) satellite measurement to a given TCCON measurement, we can safely assume that the distribution of datapoints within the 250 km radius circle is not going to be uniform, nor for that matter is the collocation area often a perfect circle (islands, coasts, mountain ranges etc.). So in stead of defining a geometrical threshhold that encapsulates 68% of the area (at a radius of 205 km for a 250 km radius circle), we ranked our collocated data according to the sat-TCCON distance and determined the lowest distance value that is at least as high as 68% of the distances sampled. For the CO2_OC2_FOCA algorithm this corresponded with 166 km. For CO2_TAN_OCFP the distance found was 164km. Both of them very similar. The CH4_S5P_WFMD datapoints on the other hand are collocated far closer to the TCCON location; on average 68% of the collocated was measured within a

34.3 km radius.

For the CO2_OC2_FOCA algorithm the bias increases by 0.18 ppm per 100 km (see **Figure 2**). This would correspond with a spatial collocation_error ($\sigma_{Collocation}$) of 0.30 ppm. For Tansat OCFP XCO_2 we can likewise derive a slope of 0.35 ppm / 100 km which would yield a standard deviation of 0.57 ppm. The latter number is derived from a far smaller data sample, but even so the uncertainties on both slopes do not overlap. This immediately highlights the limitations of our estimate, as, in theory, the evolution of the bias as a function of distance should be independent of the algorithms employed. Having more confidence in the CO2_OC2_FOCA assessment (number of data) we will use the 0.18 ppm / 100 km dependece which also results in a 0.30 ppm collocation error for our rough assessment of the impact of the collocation error.

Likewise for the CH4_S5P_WFMD algorithm we obtain a slope of -4.84 ppb / 100 km or a spatial collocation error (1 sigma) of 1.7 ppb.

To verify the stability of the algorithm over time we fit a linear trend over all collocated datapair sat-fts differences as a function of time. To check if no hemispherical component is at play we also performed the same analysis for Northern and Southern hemisphere only data. As such we derive a slope, the standard error thereon and the probability (p) of the slope being equal to 0.

We also fit a seasonal cycle through the bias timeseries:

$$X = i + s.t + A.\sin(2\pi.(t + ph)) \qquad (4.5)$$

Here, X represents the satellite minus TCCON difference, i the intercept, s the slope which corresponds with the linear drift, A the amplitude of the seasonal cycle and ph the phase shift. While the slope yields information on any potential drift, the amplitude in the above fit results gives us information on the potential mismatch between Satellite and TCCON seasonal cycles. Ideally there should be no difference between these cycles which would yield an amplitude=0 in the bias timeseries. The observed amplitude in the bias can be a direct result of either different amplitudes in the seasonal cycle of the individual data or a shift in the phase of the seasonal cycle. We therefore also fitted the same function through the individual satellite and TCCON datapoints and looked at the parameter differences.

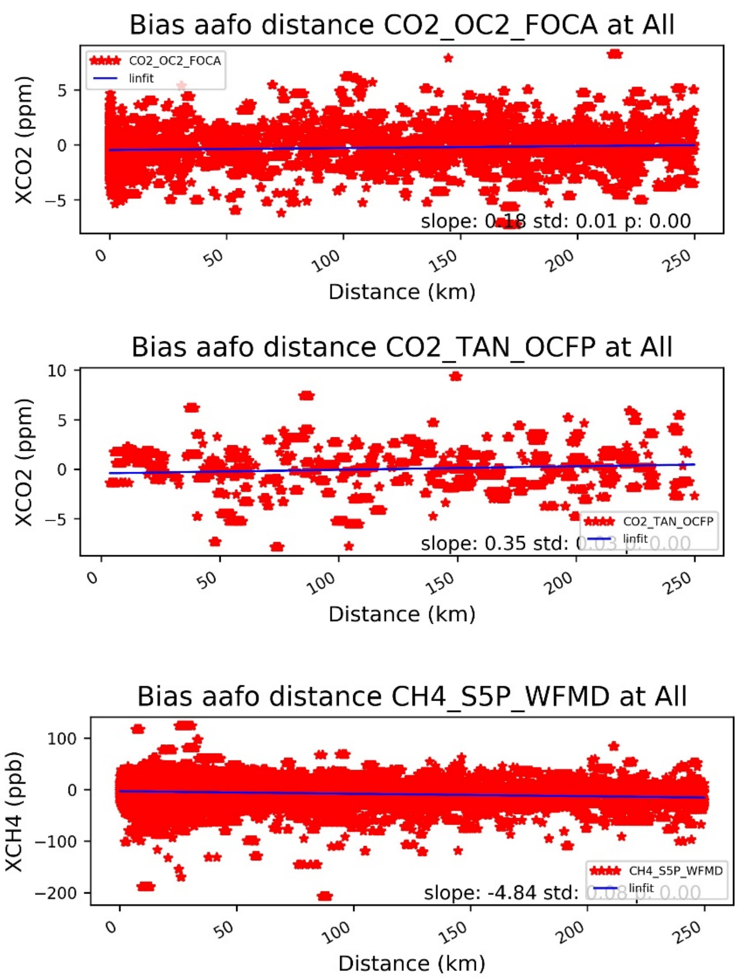

Figure 2: Satellite-TCCON bias as a function of (aafo) distance between the satellite and TCCON sampling point, using all collocated data for CO2_OC2_FOCA (top), CO2_TAN_OCFP (mid) and CH4_S5P_WFMD (bottom). Slope in ppm/100 km for XCO_2 and ppb/100 km for XCH_4.

4.2 Validation results

This section lists all validation results for the algorithms presently available in this study. First we show, for each algorithm, a general overview of the (daily averaged) collocated data.

This comprises of a Taylor plot and a mosaic overview of the obtained timeseries.

The Taylor plot shows the correlation between the various TCCON sites and the retrieval algorithm, the standard deviation of the TCCON data at each site, relative to the standard deviation of the satellite (normalized to 1) and the root mean square error of the sat-fts difference.

We also discuss aspects of collocation and temporal variability (in terms of long term stability as well as the capability of the retrieval algorithm to accurately capture the seasonal cycle.

After this we discuss the FoM, obtained from the analysis of individual data, and their statistical reliability.

Thus in each section we show:

1) A Taylor and Mosaic overview plot.
2) A table listing all Bias, Scatter, correlation (R) and number of daily averaged collocated data pairs (N) for all stations.
3) Example plots of collocation areas.
4) Example timeseries.
5) Plots outlining the temporal stability of the algorithm featuring a linear fit through the bias data, a seasonal fit through the bias data and seasonal fits through the original data.
6) A Summary table of the Figures of Merit drawn from the individual datapairs, using (non high altitude) stations which harbor sufficient data.

4.2.1 Validation results for product CO2_OC2_FOCA

Below we show the validation results of the XCO_2 concentrations as derived by the CO2_OC2_FOCA algorithm using OCO-2 spectra. Data was available from January 2015 until the end of 2018.

4.2.1.1 Detailed results

The Taylor diagram below in **Figure 3** yields a concise overview of the capabilities of the CO2_OC2_FOCA algorithm. Most TCCON sites cluster between the 0.8 and 0.9 correlation line. Also, the normalized standard deviation of most sites is close to 1, indicating that the variability of both datasets (due to natural variability and random error) is comparable. The normalized standard deviation of the bias (std(sat-fts)/std(sat)) sits (for most sites) between 0.4 and 0.6, which is encouraging as it suggests that a large fraction of the variability (we can only assume it is the natural variability part) within the TCCON timeseries is also captured by the satellite.

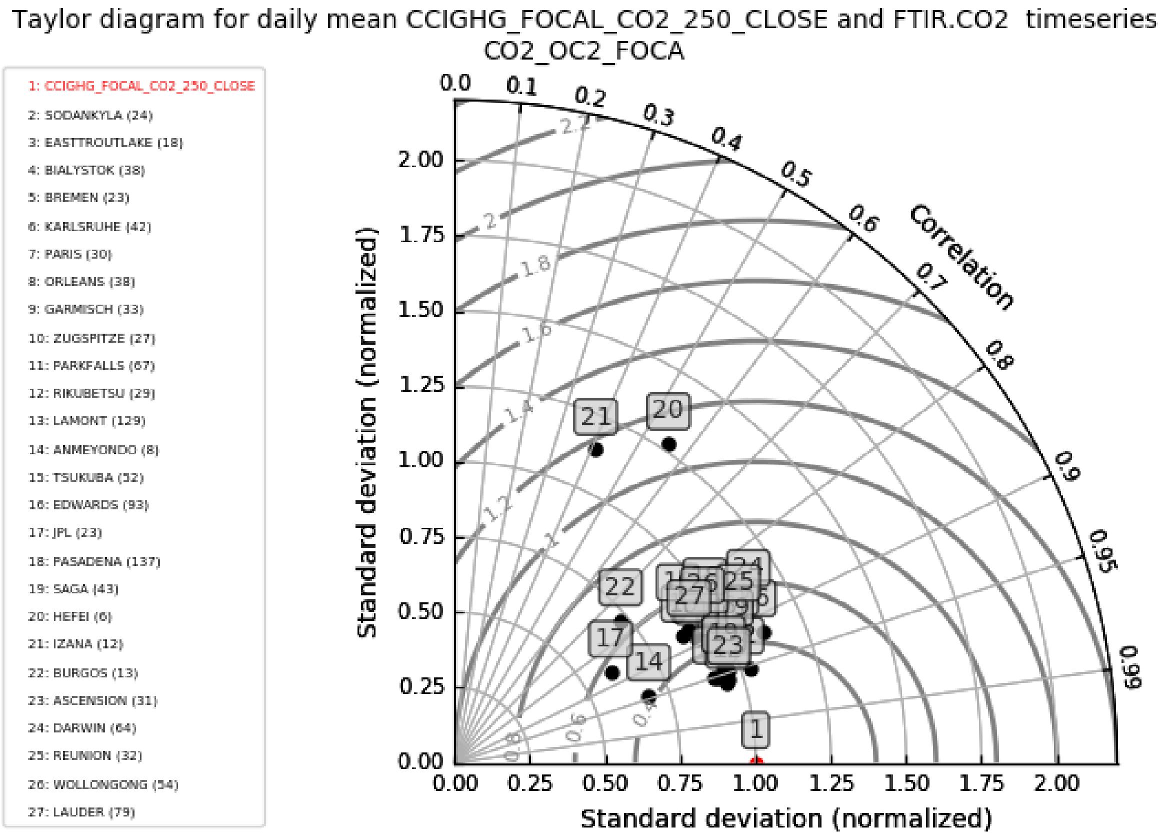

Figure 3: Tayor plot of daily averaged XCO_2 TCCON values relative to CO2_OC2_FOCA.

Notable outliers are Izaña (mountain site) and Hefei (very small dataset). JPL (California) with much lower correlations and higher scatter, Anmeyondo (Korea) and to a lesser degree Burgos, show a normalized standard deviation between 0.75 and 0.5, which could indicate that they are less sensitive to the natural variability as seen in the satellite data.

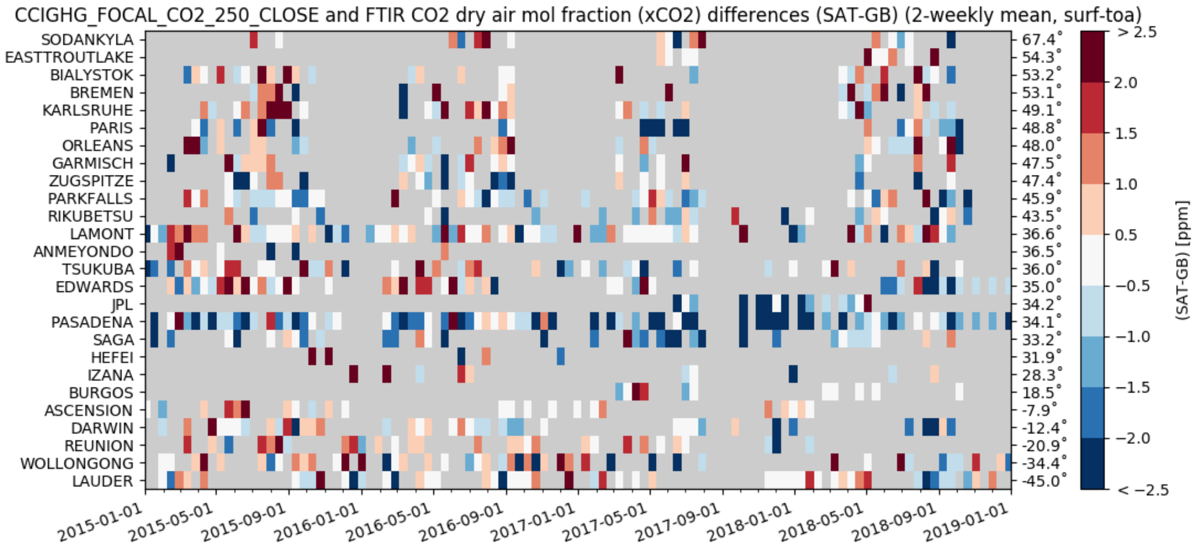

Figure 4. Mosaic plot of bi-weekly mean TCCON - CO2_OC2_FOCA XCO_2 biases as a function of time and TCCON station.

It is hard to discern a pattern in the above mosaic plot (**Figure 4**), which shows the mean bi-weekly bias between the satellite and TCCON measurement pairs. One can see the seasonal unavailability of data during winter (not visible for the Southern hemisphere as Lauder (New Zealand) still sits at a modest 45°S. JPL and nearby Pasadena appear have the strongest negative biases (see also **Table 3**). Biases could be due to actual satellite vs. TCOON differences but also due to collocation mismatches. To assess the latter we have plotted a map of the actual collocation locations and corresponding bias (**Figure 5**). The larges biases (see **Table 3**) are observed at Saga, Easttroutlake, Paris and Pasadena/JPL,

For the latter, this is not surprizing as it is located within the Los Angeles basin and typically measure larger concentrations than what is present outside the basin. However, if we look at the actual bias maps (**Figure 5**) the difference is not as clear, with low bias values within the basin as well as outside. Inclusion or rejection of these sites has an impact on the relative accuracy estimates shown in the summary table. Here we have opted to include as many stations as possible, if they harbour enough data. Given that they are included, one should be aware of its limitations.

Table 6: Bias, Scatter, Correlation and number of daily averaged datapair results for all TCCON sites as used in the Taylor plot analysis. Data from stations marked by a * were withheld from the FoM calculations.

	N	R	Bias	Std	latitude
SODANKYLA	24	0.95	0.35	1.58	67.4
EASTTROUTLAKE	18	0.91	0.86	1.56	54.3
BIALYSTOK	38	0.95	0.51	1.39	53.2
BREMEN	23	0.95	0.65	1.71	53.1
KARLSRUHE	42	0.92	0.77	1.68	49.1
PARIS	30	0.91	-0.78	1.72	48.8
ORLEANS	38	0.91	0.64	1.63	48.0
GARMISCH	33	0.92	0.22	1.51	47.5
ZUGSPITZE*	27	0.89	-0.85	1.71	47.4
PARKFALLS	67	0.95	-0.18	1.58	45.9
RIKUBETSU	29	0.96	-0.58	1.26	43.5
LAMONT	129	0.87	0.17	1.93	36.6
ANMEYONDO*	8	0.94	-0.30	2.13	36.5
TSUKUBA	52	0.88	-0.19	1.83	36.0
EDWARDS	93	0.83	0.33	2.28	35.0
JPL	23	0.86	-1.03	2.14	34.2
PASADENA	137	0.85	-1.25	2.06	34.1
SAGA	43	0.94	-1.21	1.45	33.2
HEFEI*	6	0.56	0.39	3.05	31.9
IZANA*	12	0.41	-0.19	2.34	28.3
BURGOS	13	0.76	0.03	1.38	18.5
ASCENSION	31	0.96	0.52	0.77	-7.9
DARWIN	64	0.88	-0.27	1.72	-12.4
REUNION	32	0.89	0.46	1.19	-20.9
WOLLONGONG	54	0.86	0.04	1.80	-34.4
LAUDER	79	0.87	0.03	1.50	-45.0
Mean	--	0.87	-0.03	1.73	

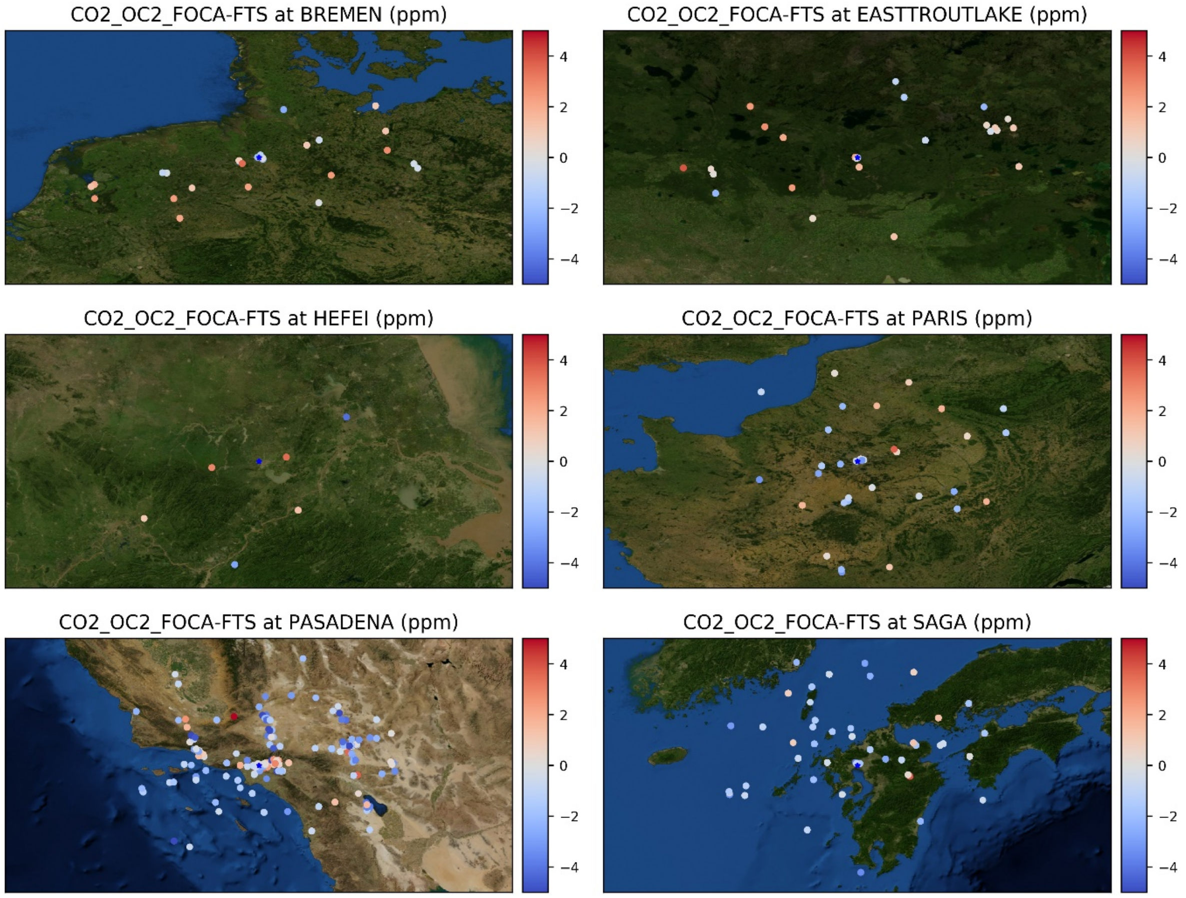

Figure 5: Bias (sat-fts) (ppm) of individual collocation points as a function of location for Bremen, Easttroutlake, Hefei, Paris, Pasadena and Saga.

The example timeseries below in **Figure 6** show individual satellite and ground-based fts measurements. Capture of the seasonal cycle, stability and uncertainty look similar to that of TCCON, for Karlsruhe even exhibiting far less outlier values. We can also indeed see the slight negative bias at the Pasadena TCCON site.

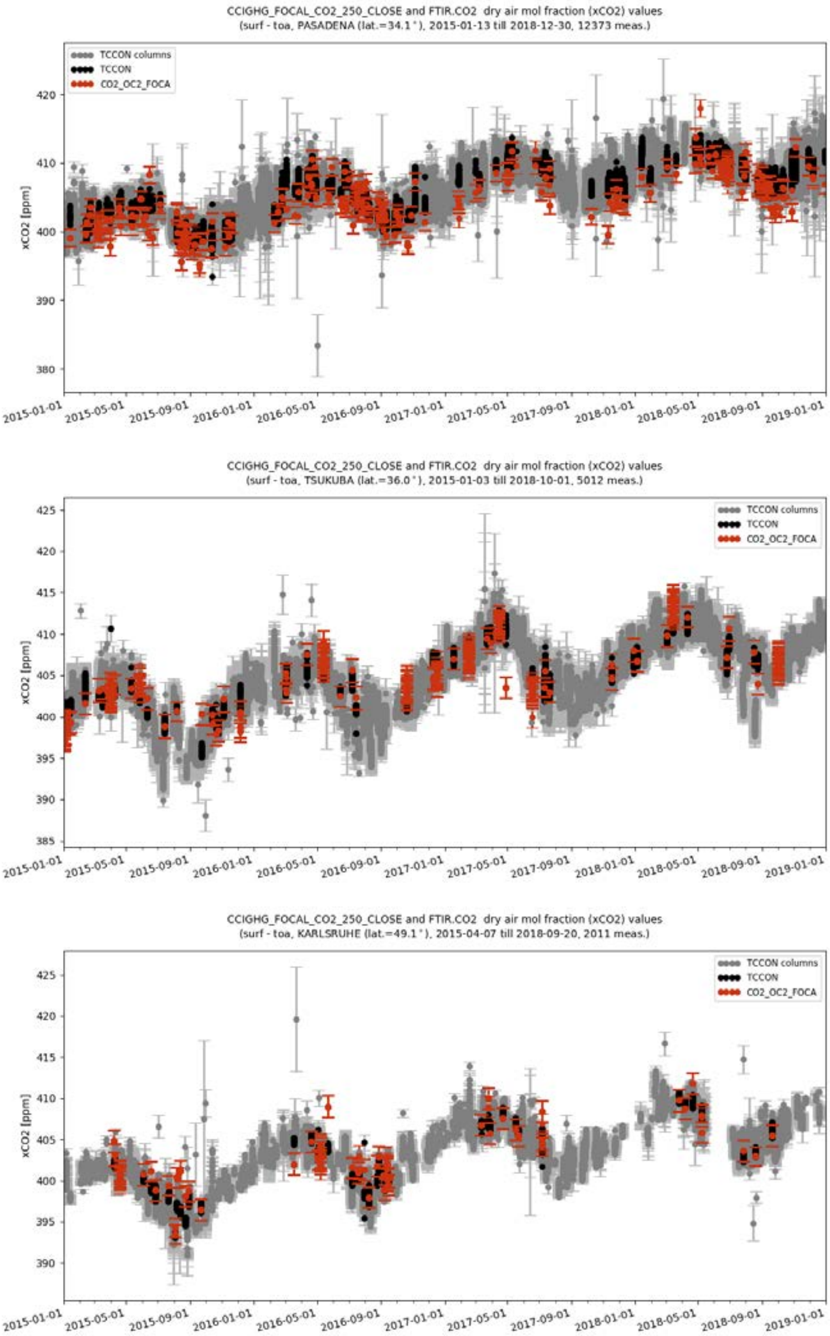

Figure 6: Example XCO_2 timeseries at Pasadena, Tsukuba and Karlsruhe (red= CO2_OC2_FOCA data, black is collocated TCCON data and grey are the uncollocated TCCON data).

When we take all datapairs, the evolution of the bias shows a small decreasing trend (-0.16 ± 0.06 ppm/year) that apears to be significant (probability of a slope=0 is 1% (p=0.01)). Also there appears to be a slight but noticeable seasonal cycle in the bias data. When fitting a seasonal function through the individual TCCON and CO2_OC2_FOCA datasets, we see that the observed amplitude in the bias is mainly due to a slightly different amplitudes in the individual fits (difference of 0.27 ppm), since there is very little difference in the phase (5 days).

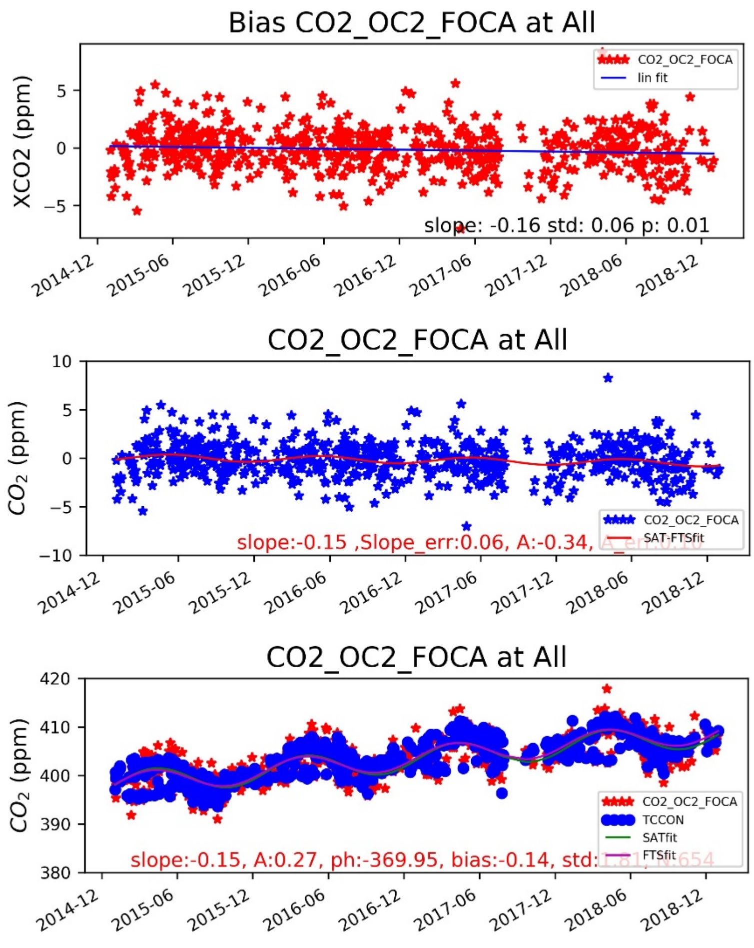

Figure 7: Daily averaged sat-fts datapair values (bottom) and differences (top,mid) as a function of time, fitted by a linear regression routine (top) and a seasonal fit (mid, bottom). The slope, phase and Phase (Ph) numbers notated in the bottom plot correspond with the sat-TCCON fit difference.

However as can be seen in **Table 4** below, which lists the results of All data, Northern and Southern hemisphere only and the 3 stations that feature the most data (Lamont, Pasadena and Lauder), there are ample of station to station differences. In fact, slopes at different stations range between 2.24 and -0.65 ppm/year. Previous analysis included alternative ways of calculating the overall trend, relying on a weighted average of the individual slope fits at each station. Typically this yielded similar overall stability results but with a larger uncertainty. We did not persue this method in this analysis as the individual fits employed on stations with limited datapoints, yielded erratic results.

Table 7: Assessment of the overall long term stability determined by fitting a linear (black) and linear + seasonal (red) function through the data. P= the probability that the real slope as derived from the linear regression equals 0, A=amplitude of the seasonal cycle. For all, Northern and Southern hemisphere data as well as for the 3 stations that features the largest dataset.

	Slope	**P**	**A**
All	-0.16±0.06 -0.15±0.06	0.01	 0.34±0.10
NH	-0.15±0.07 -0.17±0.07	0.04	 0.64±0.13
SH	-0.28±0.09 -0.25±0.09	0.00	 0.31±0.13
LAMONT	-0.03±0.16 -0.07±0.16	0.84	 0.76±0.26
PASADENA	-0.27±0.15 -0.33±0.15	0.06	 0.60±0.26
LAUDER	0.00±0.15 0.06±0.16	0.98	 0.39±0.24

4.2.1.2 Summary

Listed in the table below (**Table 8**) are the Figure of Merit parameters as derived from the individual datapairs. Hefei and Anmeyondo yielded too little data to be included in the FoM calculations.

Also important to note is that the results not only pertain to the actual data quality but also contain a collocation error component. For instance the difference in the observed bias at the relatively close by Pasadena and Edwards station is almost 0.9 ppm.

Overall the CO2_OC2_FOCA product delivers data that matches very well with that of TCCON. It does not meet the accuracy requirements of < 0.5 ppm, but again this target assumes the abolishment of any collocation influence. The standard deviation on the bias is considerably smaller than the individual biases on the satellite and TCCON datasets respectively.

The dataset shows a small but significant negative slope and has a fairly accurate error estimate.

Table 5 presents an overview of the estimated data quality as obtained from comparisons with TCCON ground-based reference observations. Values in square brackets [ ] correspond with the upper and lower 95% confidence bound on the parameter. The uncertainty ratio features 2 numbers as outlined in the validation method.

Table 8: Summary validation of product CO2_OC2_FOCA by the independent validation team using TCCON ground-based reference data. Figures in brackets show the 95% confidence bonds.

Product Quality Summary Table for Product: CO2_OC2_FOCA Level: 2, Version: v08, Time period covered: 1.2015 – 12.2018 Assessment: Validation Team (VALT)			
Parameter [unit]	**Achieved performance**	**Requirement**	**Comments**
Single measurement precision (1-sigma) in [ppm]	1.94 [1.93,1.95]	< 8 (T) < 3 (B) < 1 (G)	Computed as standard deviation of the difference to TCCON
Uncertainty ratio [-]: Ratio reported uncertainty to standard deviation of satellite-TCCON difference	0.64, 0.68*	-	No requirement but value close to unity expected for a high quality data product with reliable reported uncertainty.
Mean bias (global offset) [ppm]	-0.25 [-0.27,-0.24]	-	No requirement but value close to zero expected for a high quality data product.
Accuracy: Relative systematic error [ppm]	Spatial: 0.73 [0.54,1.01] Spatio-temporal: 0.96 [0.82,1.12]	< 0.5	Spatial: Computed as standard deviation of the biases at the various TCCON sites. Spatio-temporal: As "Spatial" but also considering seasonal biases.
Stability: Drift [ppm/year]	-0.16 +/- 0.06 P=0.0087 (1-sigma)	< 0.5	Linear drift

4.2.2 Validation results for product CO2_TAN_OCFP

Here the 250 km, 2 hour collocation criteria, struggled to obtain enough data for our analysis and as a result the FoM are far less robust. We did a test with relaxed spatial criteria (500 km), but this this yielded little more data, so we retained the original 250 km criteria to be consistent with the other algorithms.

4.2.2.1 Detailed results

The Taylor diagram below in **Figure 8** shows a short overview of the capabilities of product CO2_TAN_OCFP. Most TCCON sites cluster around the 0.6 correlation line. Also the normalized standard deviation of most sites is smaller than 1, indicating that the variability of the TCCON data is smaller. The normalized standard deviation of the bias sits (for most sites) around 0.8. Notable outliers are Karlsruhe and Sodankyla, with much larger TCCON variability and Burgos with negative correlation (probably due to the very limited amount of data). All this indicates that while OCFP data features a stronger variability (random error and/or seasonal variability) than the TCCON data, the daily mean biases still harbour less variability then either of them, an indication of OCFP capturing the natural variability.

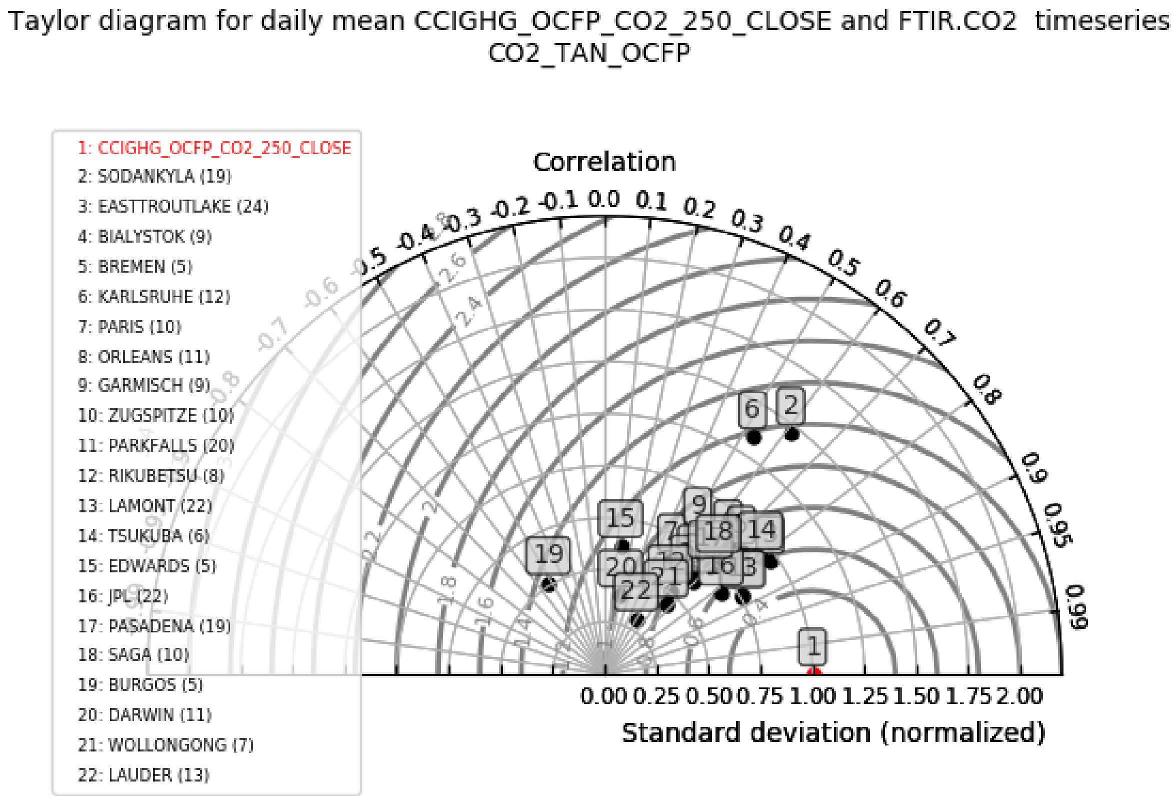

Figure 8: Tayor plot of daily averaged XCO_2 TCCON values relative to product CO2_TAN_OCFP.

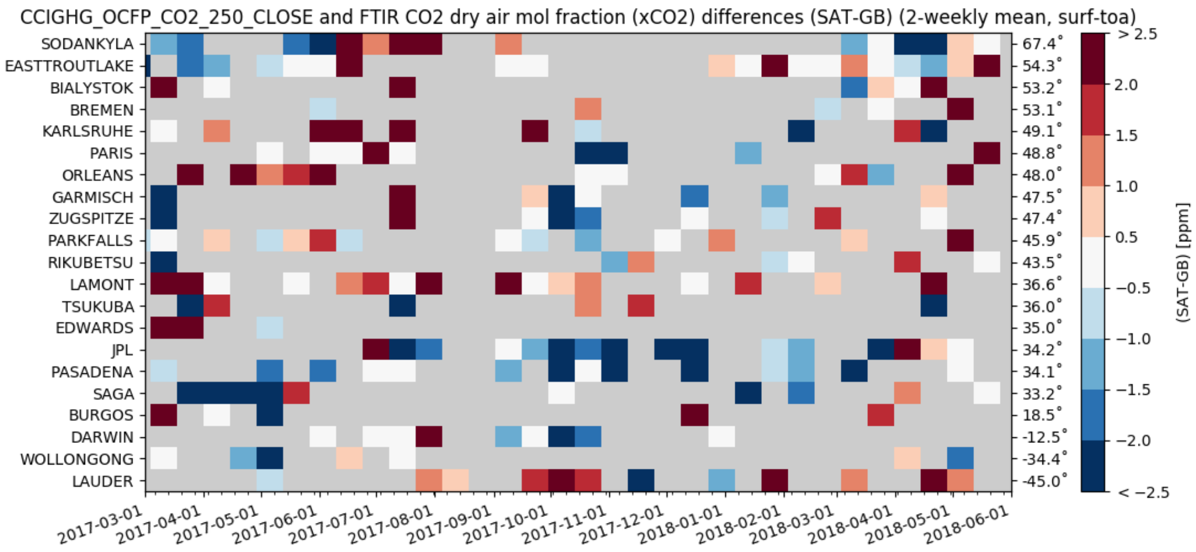

Figure 9: Mosaic plot of bi-weekly mean TCCON-WFMD XCH4 biases as a function of time and TCCON station.

Again there is no discernible pattern in the above mosaic plot (**Figure 9**), which shows the mean bi-weekly bias between the satellite and TCCON measurement pairs. However the number of data points that make up the above plot is very limited, with the highest amount of daily averaged data pairs being a mere 22 pairs (Lamont and JPL). This results in validation parameters which are far less robust than the ones obtained from the CO2_OC2_FOCA dataset. Often, such as with linear regression and fitting results, the obtained uncertainties do not reflect the actual underlying uncertainty either.

Table 6 lists all bias and scatter results derived from daily datapairs as shown in the Taylor plot above. The observed mean bias ranges between 1.99 ppm (Edwards) and -1.73 ppm (Pasadena), while the evolution of the bias as a function of distance (not shown) was the largest for Orleans and Paris. In both cases the extremes are stations that are in fair proximity to one another, with overlapping collocation areas (as shown in **Figure 10**). Again we opted to include as many stations as possible in the FoM calculations but the minimal 10 individual satellite measurement threshold resulted in a substantial reduction of our station dataset (Stations marked with *, were not used for the FoM calculations). In the end the following stations were used in the FoM: Sodankyla, Easttroutlake, Karlsruhe, Paris, Orleans, Parkfalls, Garmisch, Lamont, JPL, Pasadena, Darwin and Lauder.

Table 9: Bias, Scatter, Correlation and number of daily averaged datapair results for all TCCON sites as used in the Taylor plot analysis. Data from stations marked by a * were withheld from the FoM calculations.

	N	R	Bias	Std	latitude
SODANKYLA	19	0.61	-0.89	4.04	67.4
EASTTROUTLAKE	24	0.83	0.03	1.69	54.3
BIALYSTOK*	9	0.69	1.13	2.97	53.2
BREMEN*	5	0.75	0.82	2.06	53.1
KARLSRUHE	12	0.53	1.12	2.87	49.1
PARIS	10	0.51	0.08	2.57	48.8
ORLEANS	11	0.64	1.61	2.12	48.0
GARMISCH	9	0.55	-0.35	2.70	47.5
ZUGSPITZE*	10	0.69	-0.61	2.52	47.4
PARKFALLS	20	0.87	-0.32	1.74	45.9
RIKUBETSU*	8	0.62	-0.64	2.39	43.5
LAMONT	22	0.87	1.58	1.51	36.6
TSUKUBA*	6	0.80	-0.73	2.62	36.0
EDWARDS*	5	0.12	1.99	1.95	35.0
JPL	22	0.82	-0.70	2.24	34.2
PASADENA	19	0.70	-1.73	1.98	34.1
SAGA*	10	0.71	-1.53	1.98	33.2
BURGOS*	5	-0.53	0.90	3.10	18.5
DARWIN	11	0.20	-0.04	1.94	-12.5
WOLLONGONG*	7	0.67	-0.78	1.84	-34.4
LAUDER	13	0.50	1.63	2.85	-45.0
MEAN		0.58	0.12	2.37	

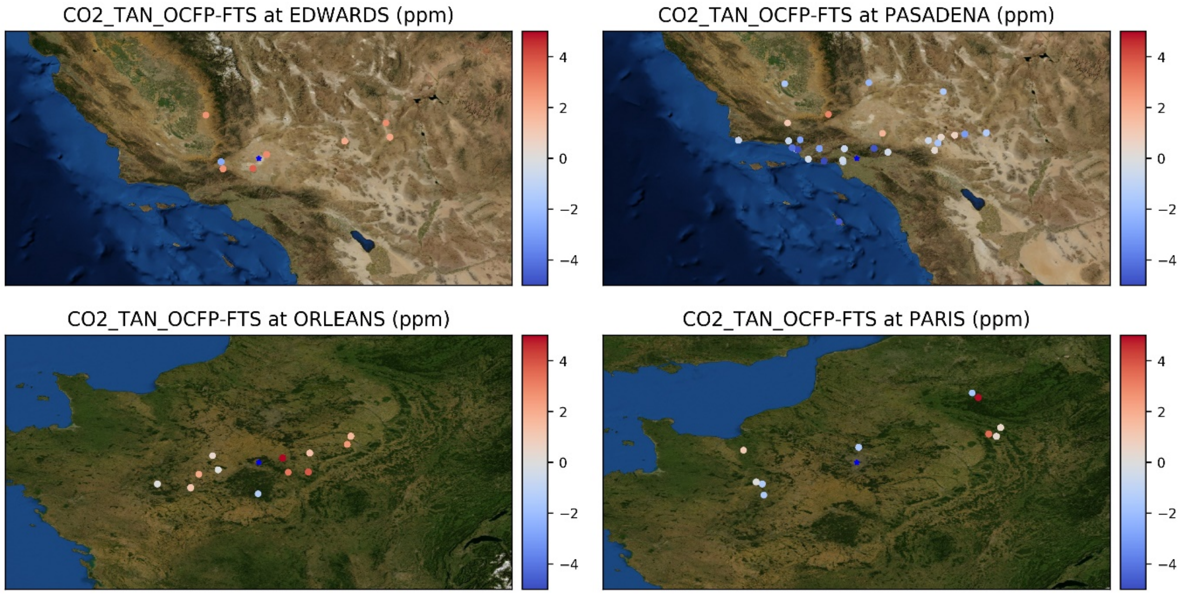

Figure 10: Bias (sat-fts) (ppm) of individual collocation points as a function of location for Edwards, Pasadena, Orleans and Paris.

The example timeseries below in **Figure 11** show individual satellite and ground-based fts measurements. Capture of the seasonal cycle, looks reasonable, but the dataset remains sparce, certainly when taking into account that the stations shown (Easttroutlake, Parkfalls and JPL) are among the stations with the highest number of collocations.

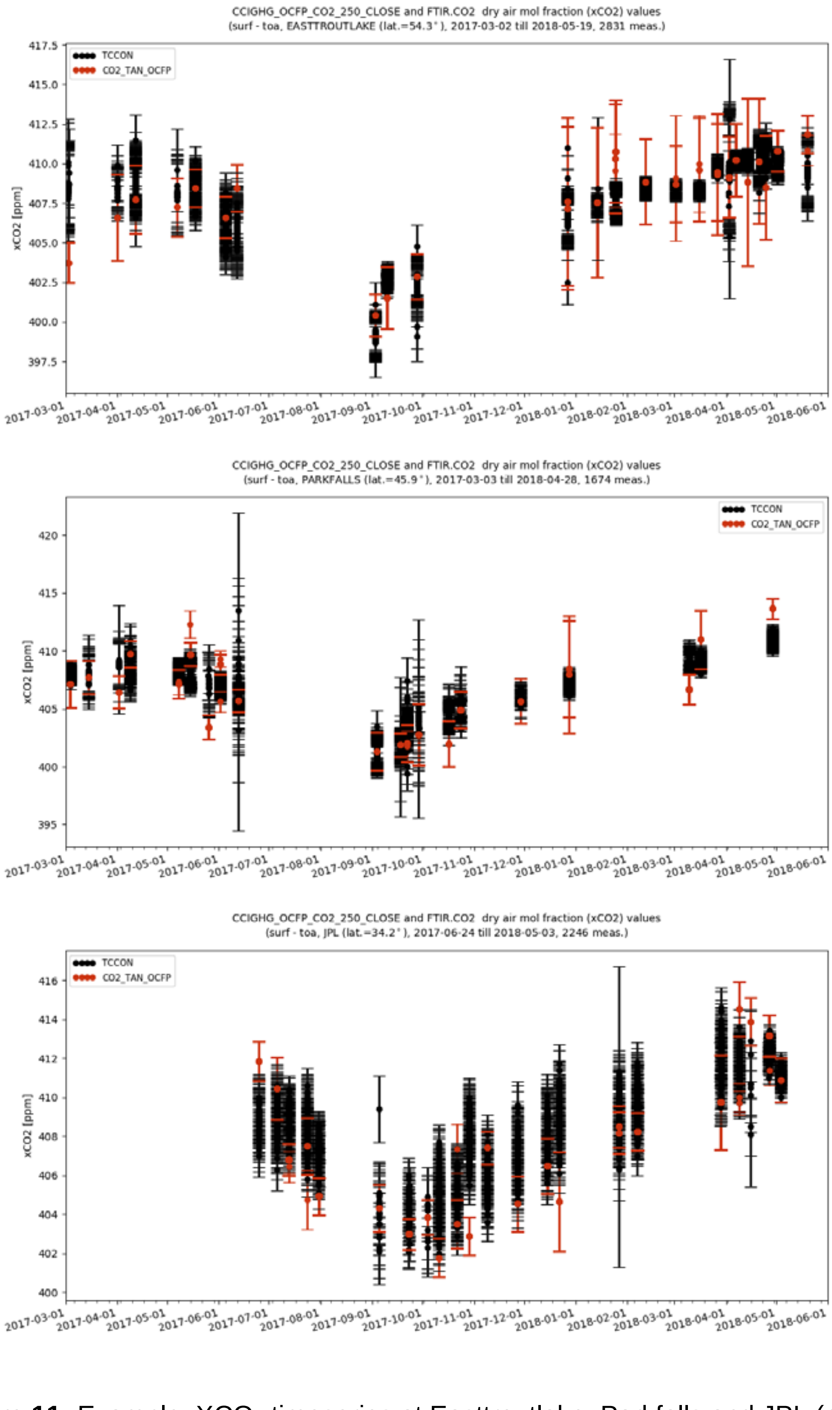

Figure 11: Example XCO_2 timeseries at Easttroutlake, Parkfalls and JPL (red= OCFP satellite data, black is collocated TCCON data.

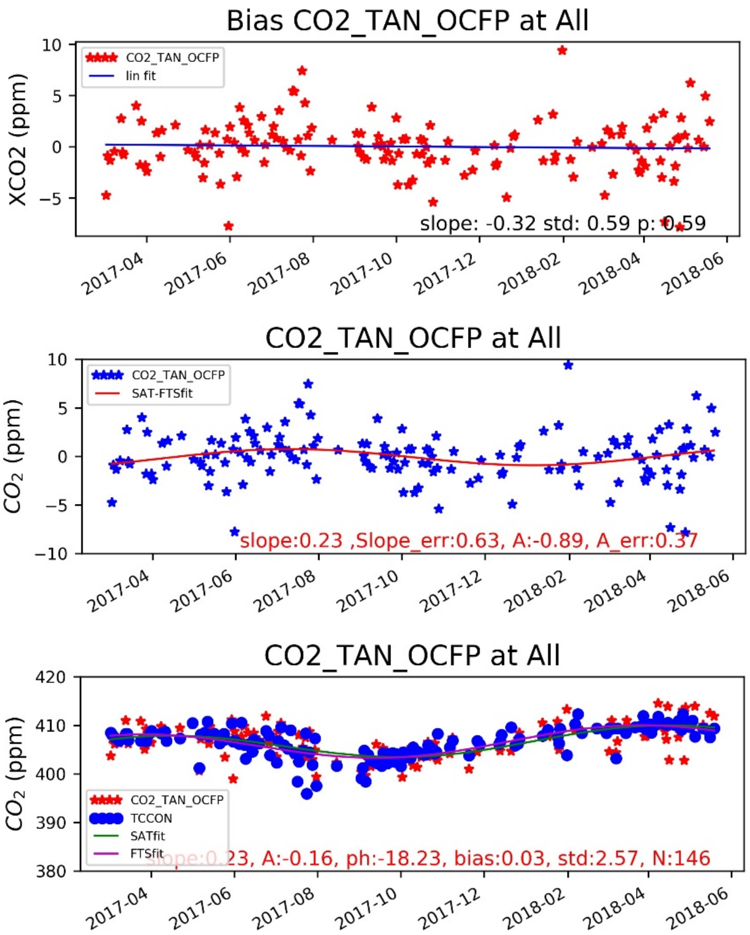

Figure 12: Daily averaged sat-fts datapair values (bottom) and differences (top,mid) as a function of time, fitted by a linear regression routine (top) and a seasonal fit (mid, bottom). The slope, phase and Phase (Ph) numbers notated in the bottom plot correspond with the sat-TCCON fit difference.

To determine the long term stability we have again fitted a linear (**Figure 12 top**) and linear+seasonal (**Figure 12 middle**) function through the data. As can be seen, there is considerable uncertainty on the terms with a linear fit p-value (probability of no slope=0.59). Also note that there is considerable difference in the slope values determined by both methods. This is probably due to the fact that the CO2_TAN_OCFP dataset does not cover a 12 month period, instead running from March 2017 until and including May 2018. This induces a potential seasonal component in the bias and thus a difference in the obtained slope.

There is also considerable difference between the Southern Hemisphere and Northern hemisphere values, but here again the extremely limited Southern hemisphere dataset, does not allow for any confident conclusions.

As FoM we have in this case opted for the value derived from the seasonal plot. CO2_TAN_OCFP appears to have a stronger seasonal cycle in its residuals (**Figure 12 middle)** than CO2_OC2_FOCA but keep in mind that the difference in time covered and stations included in the analysis. Looking at **Figure 12 bottom** the actual difference in amplitude is very small (A difference =-0.16), but we observe a 18 day difference in the phase.

Table 10: Assessment of the overall long term stability determined by fitting a linear (black) and linear + seasonal (red) function through the data. P= the probability that the real slope as derived from the linear regression equals 0, A=amplitude of the seasonal cycle. For all, Northern and Southern hemisphere data as well as for the 3 stations that features the largest dataset.

	Slope	P	A
All	-0.32±0.59 0.23±0.63	0.59	 0.89±0.37
NH	-0.47±0.59 0.11±0.61	0.42	 1.09±0.38
SH	2.73±2.04 2.86±2.92	0.19	 0.80±0.75
EASTTROUTLAKE	1.39±0.81 1.78±0.83	0.10	 0.94±0.55
LAMONT	-0.25±1.08 0.34±1.26	0.82	 0.62±0.47
JPL	1.15±1.76 0.37±3.09	0.52	 1.66±0.59

4.2.2.2 Summary

Despite the limited amount of collocated data and the relatively small time period covered, we can already state that we see no obvious defects embedded within the CO2_TAN_OCFP product. The estimated uncertainty is certainly reasonable (Uncertainty ratio=0.74). No discernible drift could be established and the product manages to capture the seasonal variability of XCO_2 fairly well. Accuracy numbers do not meet the requirements (yet) but here again the limited dataset hampered our analysis. Straightforward comparison between CO2_OC2_FOCA and CO2_TAN_OCFP is ill advised given the different constellation of stations on which each algorithm's FoM are based.

Table 8 presents an overview of the estimated data quality as obtained from comparisons with TCCON ground-based reference observations. Values in square brackets [ ] correspond with the upper and lower 95% confidence bound on the parameter. The uncertainty ratio features 2 numbers as outlined in the validation method.

Table 11: Summary validation of product CO2_TAN_OCFP by the independent validation team using TCCON ground-based reference data.

Product Quality Summary Table for Product: CO2_TAN_OCFP Level: 2, Version: v1, Time period covered: 3.2017 – 5.2018 Assessment: Validation Team (VALT)			
Parameter [unit]	**Achieved performance**	**Requirement**	**Comments**
Single measurement precision (1-sigma) in [ppm]	2.33 [2.30,2.36]	< 8 (T) < 3 (B) < 1 (G)	Computed as standard deviation of the difference to TCCON
Uncertainty ratio [-]: Ratio reported uncertainty to standard deviation of satellite-TCCON difference	0.71, 0.75*	-	No requirement but value close to unity expected for a high quality data product with reliable reported uncertainty.
Mean bias (global offset) [ppm]	0.04 [0.005, 0,08]	-	No requirement but value close to zero expected for a high quality data product.
Accuracy: Relative systematic error [ppm]	Spatial: 0.93 [0.61,1.46] Spatio-temporal: 1.75 [1.43,2.65]	< 0.5	Spatial: Computed as standard deviation of the biases at the various TCCON sites. Spatio-temporal: As "Spatial" but also considering seasonal biases.
Stability: Drift [ppm/year]	0.2 +/- 0.6 (1-sigma)	< 0.5	Linear drift

4.2.3 Validation results for product CO2_GO2_SRFP

First retrieval results for this product will be generated in the second year of this project. Therefore, no validation results are shown in this first version of this document.

4.2.4 Validation results for product CH4_S5P_WFMD

4.2.4.1 Detailed results

The Taylor plot for product CH4_S5P_WFMD is shown in **Figure 13**. Most FTIR sites are clustered around the rather modest 0.4 correlation line, with the standard deviation of the differences almost equal to the standard deviation of the satellite data itself, which is 33% larger than that of most TCCON sites. The low correlation originates primarily from the fact that the single observation (i.e., not averaged) timeseries at a given TCCON site vary only little compared to measurement noise etc. (for TCCON and for the satellite data; see timeseries in **Figure 16**). The presence of several (mostly negative) outliers in the data (**Figure 16**) result in a substantial impact on almost all comparison parameters. Reunion and Anmeyondo are clear outliers in this plot, but both feature extremely little data.

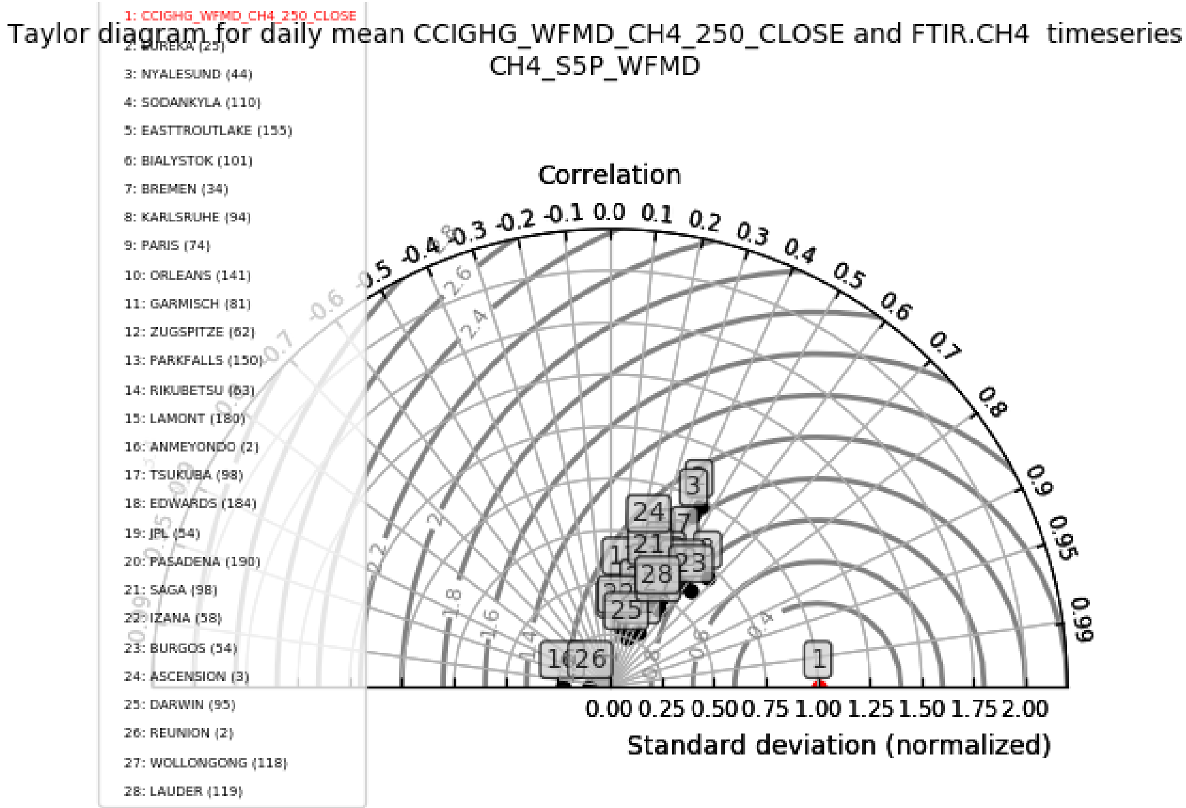

Figure 13: Tayor plot of daily averaged XCH_4 TCCON values relative to CH4_S5P_WFMD.

The mosaic overview of bi-weekly sat-TCCON biases (**Figure 14**) does not reveal any systematic trend over time, nor any as a function of latitude. There are some very pronounced biases (negative in Parkfalls and positive in Garmisch and Zugspitze), again mainly due to strong outlier values and/or high altitude stations.

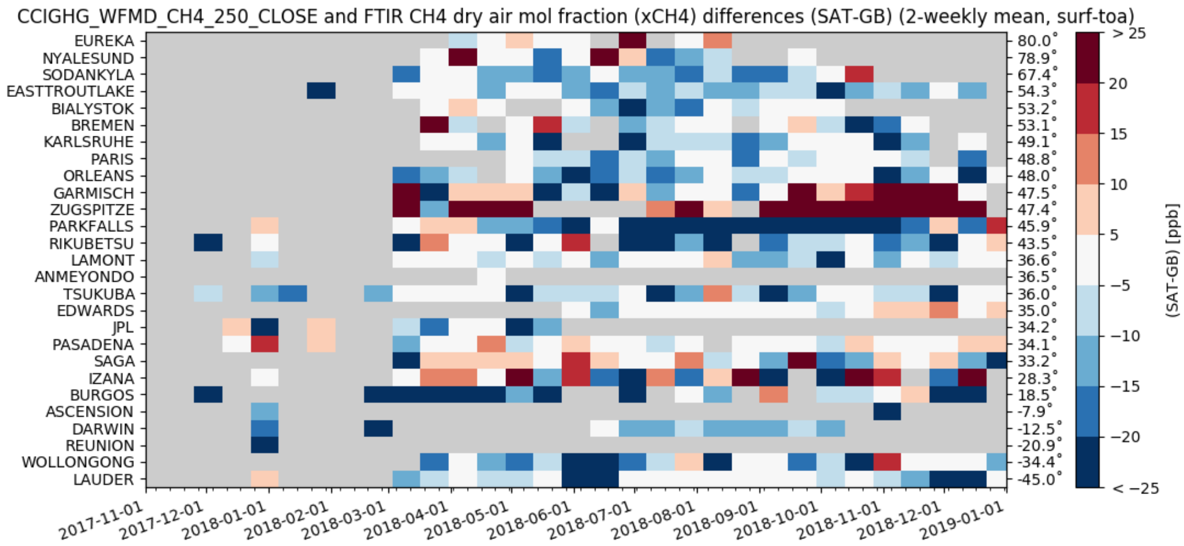

Figure 14: Mosaic plot of bi-weekly mean TCCON-WFMD XCH_4 biases as a function of time and TCCON station.

Biases differ considerably between stations, going from +41.21 (Zugspitze) to -40.61 (Reunion). The first however is a high altitude site and the latter only features 2 daily averaged TCCON-satellite pairs. If we ignore high altitude stations and those with few datapoints, the bias still ranges from -19.82 (Parkfalls) to 4.90 (Garmisch). Examples of stations and collocation biases for some of the stations that feature strong biases are shown below. Given that XCH_4 is less uniform as a function of altitude compared to XCO_2, the biases at these locations have a stronger impact. Stations that ware withheld from the figures of merit calculations are marked by an * in **Table 9**. These include Zugspitze, Izana, Ascension, Reunion and Anmeyondo. Interestingly when looking at the Garmisch tile in **Figure 15** one would expect to see the largest positive bias in the valley, at lower altitudes than the Garmisch site. However we do still see strong positive biases; near the Garmisch site, on the Alpine slopes, which again underlies the complexity of choosing ideal collocation criteria.

Table 12: Bias, Scatter, Correlation and number of daily averaged datapair results for all TCCON sites as used in the Taylor plot analysis. Data from stations marked by a * were withheld for the FoM calculations.

	N	R	Bias	Std	latitude
EUREKA	25	0.44	1.84	14.71	80.0
NYALESUND	44	0.44	2.59	18.08	78.9
SODANKYLA	110	0.45	-12.45	17.91	67.4
EASTTROUTLAKE	155	0.36	-9.64	19.58	54.3
BIALYSTOK	101	0.39	-4.66	18.18	53.2
BREMEN	34	0.49	-0.52	15.11	53.1
KARLSRUHE	94	0.66	-7.54	10.85	49.1
PARIS	74	0.49	-7.75	13.75	48.8
ORLEANS	141	0.48	-10.93	19.46	48.0
GARMISCH	81	0.46	4.90	31.56	47.5
ZUGSPITZE*	62	0.27	41.21	29.55	47.4
PARKFALLS	150	0.14	-19.82	23.66	45.9
RIKUBETSU	63	0.40	-9.03	27.42	43.5
LAMONT	180	0.45	-6.78	21.19	36.6
ANMEYONDO*	2	-1.00	3.91	7.17	36.5
TSUKUBA	98	0.50	-9.98	24.23	36.0
EDWARDS	184	0.58	0.88	14.95	35.0
JPL	54	0.14	-8.16	32.80	34.2
PASADENA	190	0.37	-2.39	26.60	34.1
SAGA	98	0.33	0.78	25.99	33.2
IZANA*	58	0.14	0.93	29.09	28.3
BURGOS	54	0.65	-19.00	24.00	18.5
ASCENSION*	3	0.26	-18.40	6.51	-7.9
DARWIN	95	0.32	-11.72	16.38	-12.5
REUNION*	2	-1.00	-40.61	69.59	-20.9
WOLLONGONG	118	0.53	-11.44	22.64	-34.4
LAUDER	119	0.49	-4.25	20.44	-45.0
------	--	0.31	-5.85	22.27	

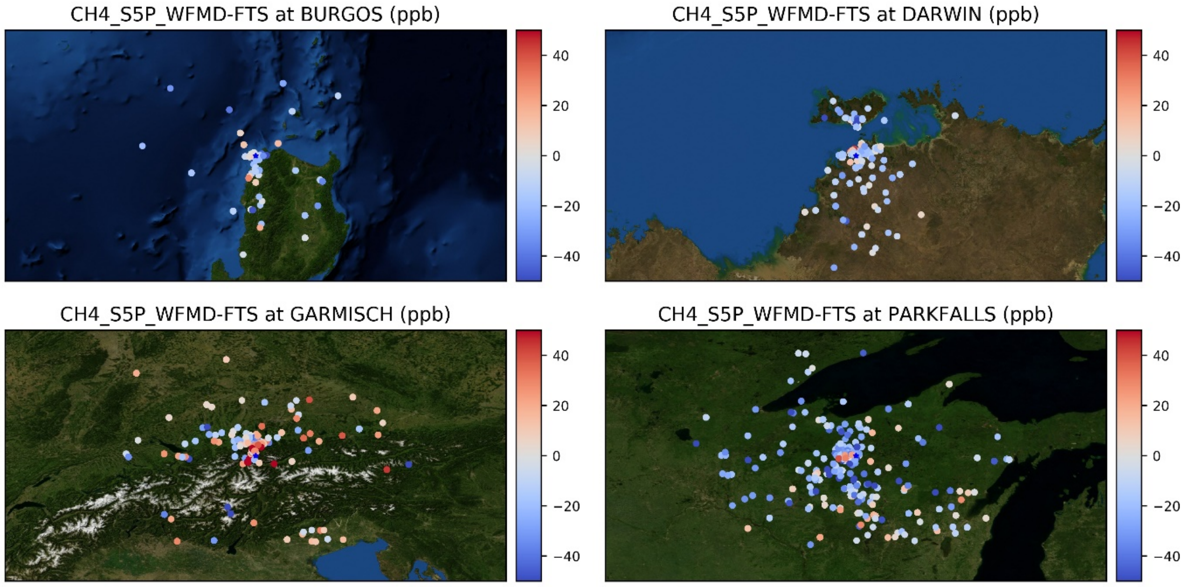

Figure 15: Bias (sat-fts) (ppm) of individual collocation points as a function of location for Burgos, Darwin, Garmisch and Parkfalls

To determine the long term stability we have again fitted a linear (**Figure 16 top**) and linear+seasonal (**Figure 16 mid**) function through the data. Due to the large scatter, any seasonal cycle (if there) is lost in the needed scale. Again we see a substantial difference between the linear and seasonal fit derived slopes (4.39 vs 6.72 ppb/year) but the errors overlap. Given that we only have 13 months of data, it is no surprise that no accurate assessment of any long term stability can be made. We observe no clear erroneous features in the timeseries as far as stability is concerned. As FoM in the summary table we have taken the slope value as derived from the seasonal fit. But it should be noted that, from the linear fit we can obtain that the slope is probably not statistically significant if we take a 95% confidence threshold (p=0.11). There is a small (Amplitude=2.44 ppb) seasonal cycle in the residual plot (**Figure 16 mid),** which is in part due to a difference in seasonal amplitude (1.4 ppb) and phase (17 days) between the WFMD and TCCON timeseries (**Figure 16 bottom**).

Table 10 shows the fitting results for all data as well as both hemispheres and (as an example) the 3 stations that feature the most data. As one can see, the trends are far from uniform and stable, both in terms of differences between stations as well as fitting method (the slope for Edwards jumps from +16.6 ppb/year to -14.1 ppb/year!) This further strengthens the fact that for an accurate evaluation the time period is too short and the scatter too large.

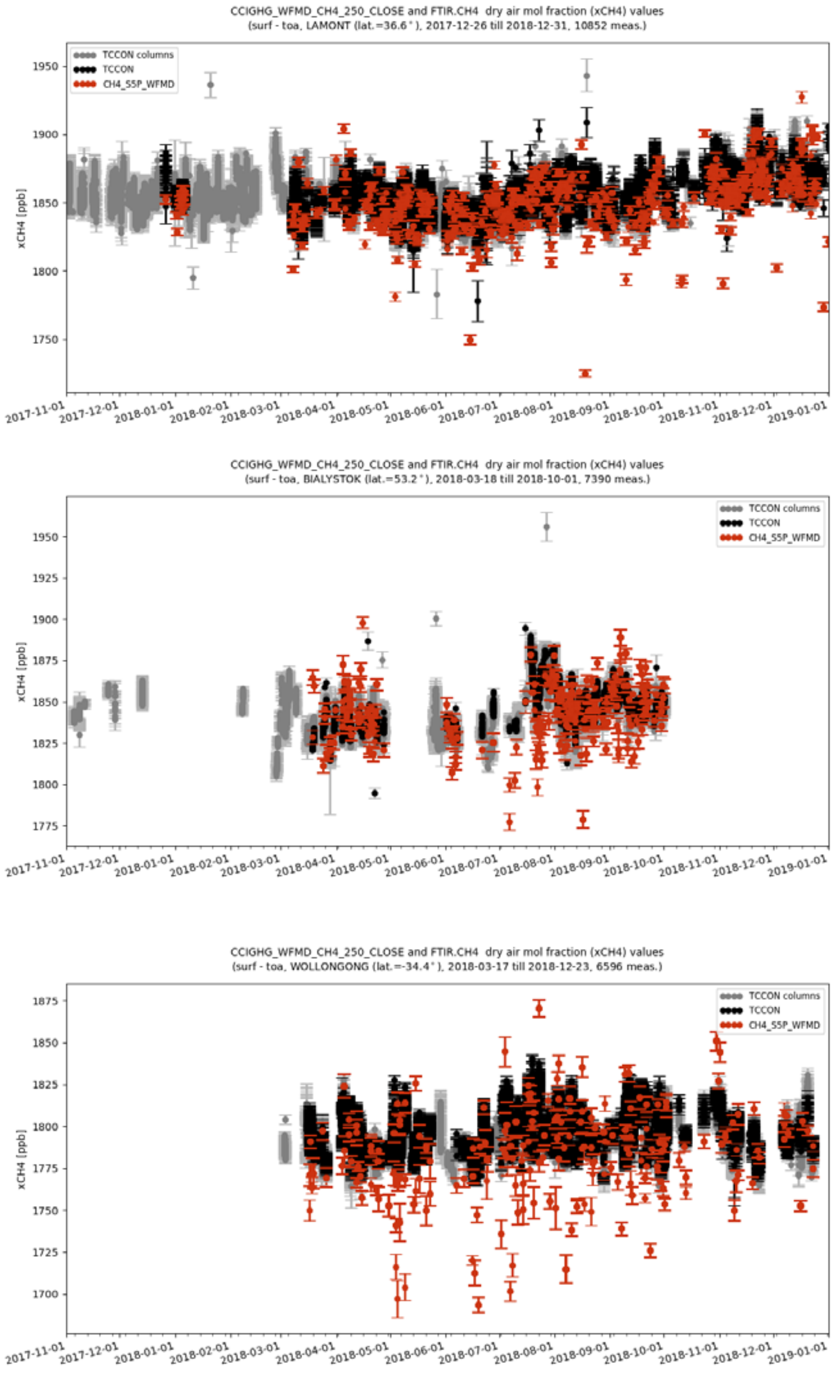

Figure 16: Example timeseries of XCH_4 TCCON (collocated=black, all=grey) and CH4_S5P_WFMD (red) data at selected TCCON sites.

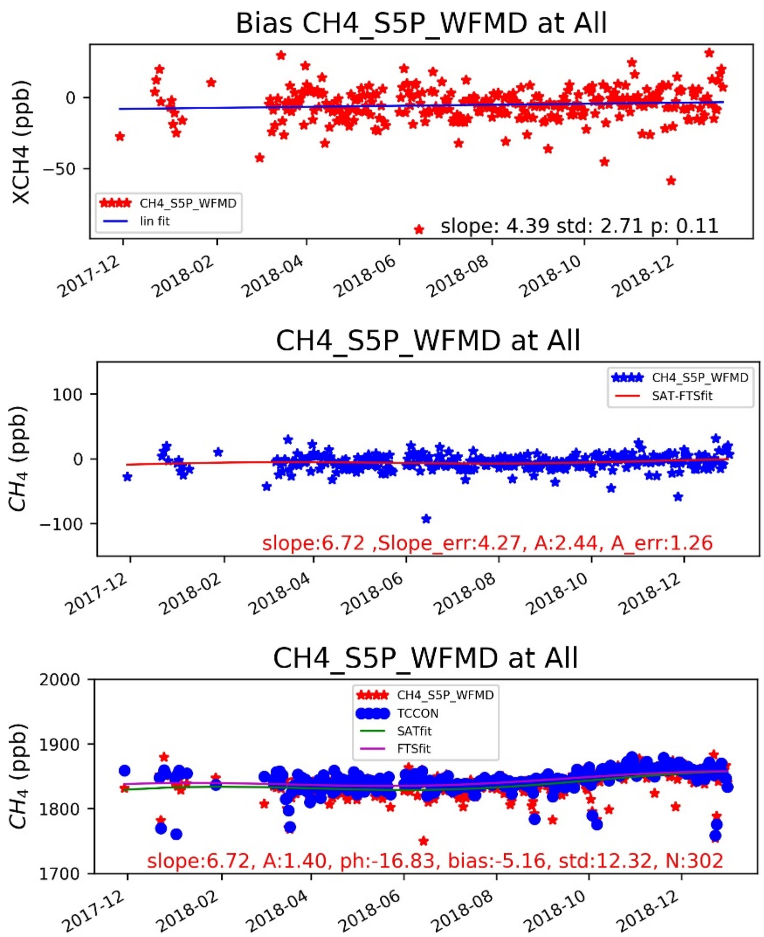

Figure 17: Daily averaged sat-fts datapair values (bottom) and differences (top,mid) as a function of time, fitted by a linear regression routine (top) and a seasonal fit (mid, bottom). The slope, phase and Phase (Ph) numbers notated in the bottom plot correspond with the sat-TCCON fit difference.

Table 13: Assessment of the overall long term stability determined by fitting a linear (black) and linear + seasonal (red) function through the data. P= the probability that the real slope as derived from the linear regression equals 0, A=amplitude of the seasonal cycle. For all, Northern and Southern hemisphere data as well as for the 3 stations that features the largest dataset.

	Slope	P	A
All	4.39±2.71 6.72±4.27	0.11	2.44±1.26
NH	5.48±2.69 8.20±4.31	0.04	2.90±1.23
SH	3.00±5.69 -10.7±10.3	0.60	5.60±3.09
LAMONT	-11.65±6.52 -5.16±10.95	0.08	3.38±3.61
EDWARDS	16.61±6.37 -14.1±37.2	0.01	7.10±8.07
PASADENA	7.36±8.98 -0.50±14.7	0.41	3.73±3.66

4.2.4.2 Summary

The CH4_S5P_WFMD data contains, unfortunately, a substantial amount of outliers (most of them negative), which severely hampers the data quality and assessed figures of merit. The single measurement precision as a result is substantial, its uncertainty ratio is far from 1, indicating a strong underestimation of its single measurement precision. Biases are likewise negative. The relative accuracy however is surprisingly (given the issues) good, with both the spatial (RA) and spatio-temporal (SRA) accuracy meeting the requirement threshold. The fact that we use median biases instead of averages to calculate the accuracy estimates certainly reduced the impact of the frequent outliers in the dataset. The table below feature an evaluation of the stability but it should be noted that at this point, the uncertainty attached to this number is probably underestimated. All analysis show that no statistically significant drift can be observed. At this point it remains unclear what causes these issues but, given that there are often strong underestimations of the observed concentrations, a prime candidate would be the failure to accurately flag cloud-contaminated observations. Once this issue is resolved, large improvements on the quality assessment figures can be expected.

Table 11 presents an overview of the estimated data quality as obtained from comparisons with TCCON ground-based reference observations. Values in square brackets [ ] correspond with the upper and lower 95% confidence bound on the parameter. The uncertainty ratio features 2 numbers as outlined in the validation method.

Table 14: Summary validation of product CH4_S5P_WFMD by the independent validation team using TCCON ground-based reference data.

Product Quality Summary Table for Product: CH4_S5P_WFMD Level: 2, Version: v1.2, Time period covered: 11.2017 – 12.2018 Assessment: Validation Team (VALT)			
Parameter [unit]	**Achieved performance**	**Requirement**	**Comments**
Single measurement precision (1-sigma) in [ppb]	20.4 [20.3,20.5]	< 34 (T) < 17 (B) < 9 (G)	Computed as standard deviation of the difference to TCCON
Uncertainty ratio [-]: Ratio reported uncertainty to standard deviation of satellite-TCCON difference	0.22, 0.23*	-	No requirement but value close to unity expected for a high quality data product with reliable reported uncertainty.
Mean bias (global offset) [ppb]	-4.84 [-4.94,-4.75]	-	No requirement but value close to zero expected for a high quality data product.
Accuracy: Relative systematic error [ppb]	Spatial: 6.50 [4.82,8.95] Spatio-temporal: 8.84 [7.57,10.38]	< 10	Spatial: Computed as standard deviation of the biases at the various TCCON sites. Spatio-temporal: As "Spatial" but also considering seasonal biases.
Stability: Drift [ppb/year]	6.7 +/- 4.3 (1-sigma)	< 3	Linear drift

4.2.5 Validation results for product CH4_GO2_SRFP

First retrieval results for this product will be generated in the second year of this project. Therefore, no validation results are shown in this first version of this document.

4.2.6 Validation results for product CH4_GO2_SRPR

First retrieval results for this product will be generated in the second year of this project. Therefore, no validation results are shown in this first version of this document.

5 Validation and intercomparisons results from data provider

5.1.1 Validation and intercomparison results for product CO2_OC2_FOCA

5.1.1.1 Comparison with CAMS model results

This section bases on section 8.1 of FOCAL's **/ATBDv1 FOCAL, 2019/** which, in turn, summarizes results of a comparison of FOCAL v06 with the CAMS model done by **/Reuter et al., 2017b/**.

Here we compare two months (April and August 2015) of post-filtered and bias corrected FOCAL v06 XCO_2 results with corresponding values of the CAMS v15r4 model accounting for FOCAL's column averaging kernels (e.g., **/Rodgers, 2000/**). **Figure 18** shows 5°×5° monthly gridded values for both months, FOCAL, and CAMS. The main spatial and temporal patterns are similar for FOCAL and CAMS with largest and smallest values in the northern hemisphere in April and August, respectively. Differences become larger at smaller scales, e.g., FOCAL sees larger values in natural and anthropogenic source regions of Sub-Saharan Africa and East Asia in April but also above the Sahara in August. However, it shall be noted that often only few data points are in the corresponding grid boxes.

In grid boxes with more than 100 soundings, the standard error of the mean becomes negligible (~0.1 ppm). Therefore, the difference between FOCAL and CAMS in such grid boxes can be interpreted as systematic temporal and regional mismatch or bias. The standard deviation of this systematic mismatch (including also representation errors) amounts to 1.0 ppm. The standard deviation of the single sounding mismatch after subtracting the systematic mismatch amounts to 1.1 ppm which agrees reasonably well with the average reported uncertainty of 1.2 ppm.

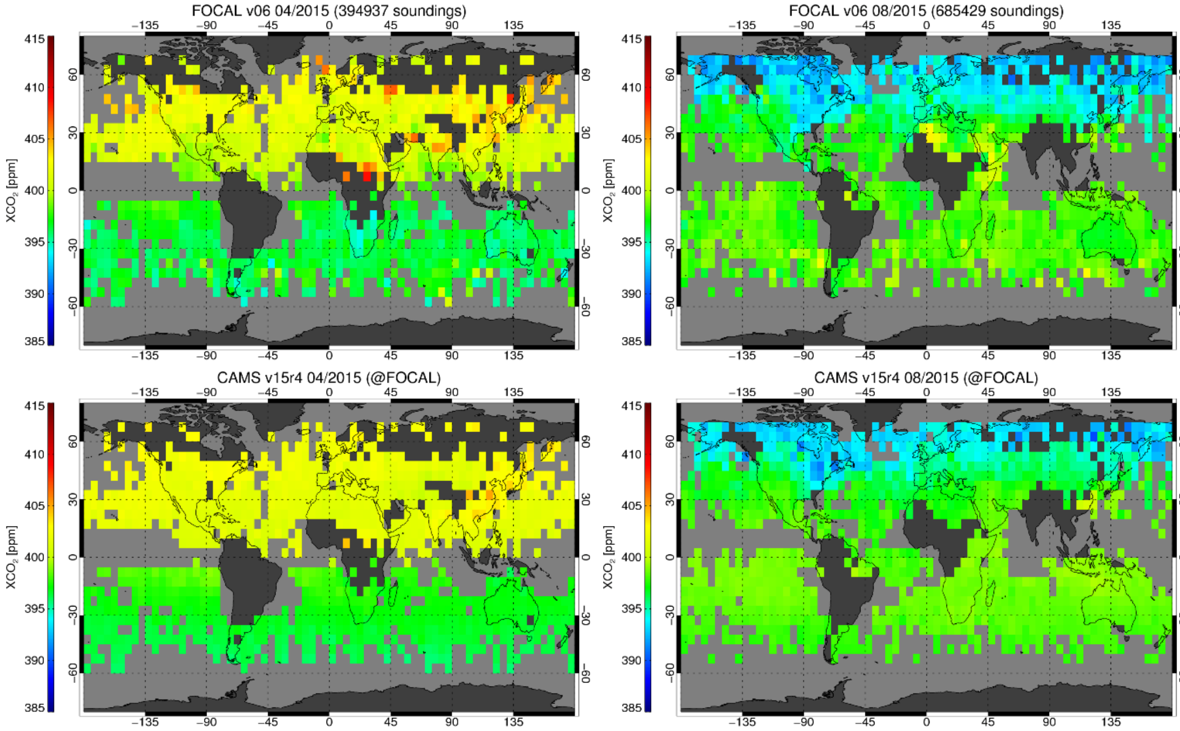

Figure 18: Monthly mean XCO_2 gridded to 5°×5°. Top: FOCAL v06. Bottom: CAMSv15r4 sampled as FOCAL. Left: April 2015. Right: August 2015.

5.1.1.2 Comparison with NASA's operational OCO-2 L2 product

This section bases on section 8.2 of FOCAL's **/ATBDv1 FOCAL, 2019/** which, in turn, summarizes results of a comparison of FOCAL v06 with the CAMS model done by **/Reuter et al., 2017b/**.

In this section we compare the same two months (April and August 2015) of post-filtered and bias corrected FOCAL v06 XCO_2 results with NASA's operational OCO-2 L2 product. Comparing **Figure 19** with **Figure 18** (top) shows similar large scale temporal and spatial patterns and also the relative enhancement in the anthropogenic source regions of East Asia in April are similar. The most obvious difference is that the NASA product has about three times more soundings. The primary reason for this is the inherently poor throughput (11%) of the MODIS based cloud screening of the preprocessor.

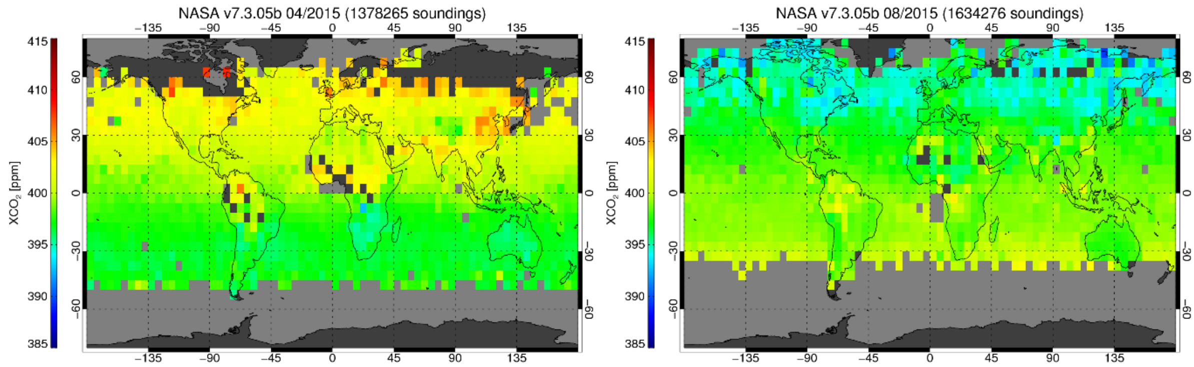

Figure 19: NASA v7.3.05b monthly mean XCO_2 at 5°×5°. Left: April 2015. Right: August 2015.

Analyzing only the same soundings in both data sets and considering the column averaging kernels, the NASA product has on average 0.7 ppm larger values than FOCAL which is (due to the used color table) most noticeable in the northern hemisphere. The standard deviation of the difference is 1.1 ppm. As done in the last section, we separate the systematic mismatch from the stochastic mismatch by analyzing grid boxes with more than 100 co-locations. The standard deviation of the stochastic and the systematic mismatch amounts 0.91 ppm and 0.83 ppm, respectively. It is no surprise, that the stochastic mismatch is smaller than expected from the combined reported uncertainties because both data products base on the same L1b input data including the same noise spectra.

5.1.1.3 Validation with TCCON

The validation results shown in this section are valid for FOCAL v08. The applied methods are similar to those described in BESD’s Comprehensive Error Characterisation Report **/CECRv3 BESD, 2017/** and the Product Validation and Intercomparison Report **/PVIRv5, 2017/** of ESA’s GHG CCI project and partly also in the publication of **/Reuter et al., 2011/**. For all comparisons, averaging kernels have been applied as described in the C3S GHG Product User Guide and Specification **/PUGS, 2019/**.

XCO_2

FOCAL’s XCO_2 has been validated with TCCON GGG2014 measurements. The co-location criteria are defined by a maximal time difference of two hours, a maximal spatial distance of 500 km, and a maximal surface elevation difference of 250 m. **Figure 20** shows all co-located FOCAL and TCCON retrievals of the years 2015-2018 for TCCON sites with more than 250 co-locations and covering a time period of at least one year. One can see that FOCAL captures the year-to-year increase and the seasonal features. For each station, the performance statistics number of co- locations, station bias, seasonal bias, linear drift, and single measurement precision were calculated.

We define the station bias as average difference to TCCON. Seasonal bias, linear drift, and single sounding precision have been derived by fitting the following trend model:

$$\Delta \boldsymbol{X} = \boldsymbol{a_0} + \boldsymbol{a_1 t} + \boldsymbol{a_2} \sin(\boldsymbol{2\pi t} + \boldsymbol{a_3}) + \boldsymbol{\varepsilon}$$

Here, ΔX represents the difference satellite minus TCCON , and a_{0-3} the free fit parameters. Specifically, a_1 represents the linear drift and a_2 the amplitude of the seasonal bias. The single sounding precision is computed by the standard deviation of the residual ε.

Based on the per station statistics, the following summarizing statistics have been calculated: Total number of co-locations used for validation, averaged single measurement precision, station-to-station bias (standard deviation of the station biases), average seasonal bias (standard deviation of the seasonal bias term), and average linear drift. As the linear drift can be assumed to be globally constant, the station-to-station standard deviation of the linear drift is a measure for its uncertainty. Per station statistics and overall performance estimates are listed in **Table 12**.

In total, ~600000 co-located FOCAL measurements have been used for the validation exercise. The overall single measurement precision is 1.52 ppm and station-to-station biases amount to 0.64 ppm.

In the context of station-to-station biases, it shall be noted that **/Wunch et al., 2010, 2011/** specifies the accuracy (1σ) of TCCON to be about 0.4 ppm. This means it cannot be expected to find regional biases considerably less than 0.4 ppm using TCCON as reference.

Seasonal cycle biases amount to 0.38 ppm on average and no significant (temporally linear) drift can be found (0.00±0.75 ppm/a).

Additionally, a measure for the year-to-year stability has been computed as follows. For each TCCON site, the residual difference (satellite - TCCON) which is not explained by station bias, seasonal bias, and/or linear drift has been derived by subtracting the fit of the bias model ΔX from the satellite minus TCCON difference. These time series were smoothed by a running average of 365 days. Only days where more than 10 co-locations contributed to the running average of at least 5 TCCON sites have been further considered. At these days, the station-to-station average has been calculated.

The corresponding expected uncertainty has been computed from the standard error of the mean (derived from the station-to-station standard deviation and the number of stations) and by error propagation of the reported single sounding uncertainties. For FOCAL, the average is always between about -0.3 ppm and 0.2 ppm (**Figure 21**) with an uncertainty of typically about 0.15 ppm. Most of the time, the average is not significantly different from zero, i.e., its one sigma uncertainty is larger than its absolute value.

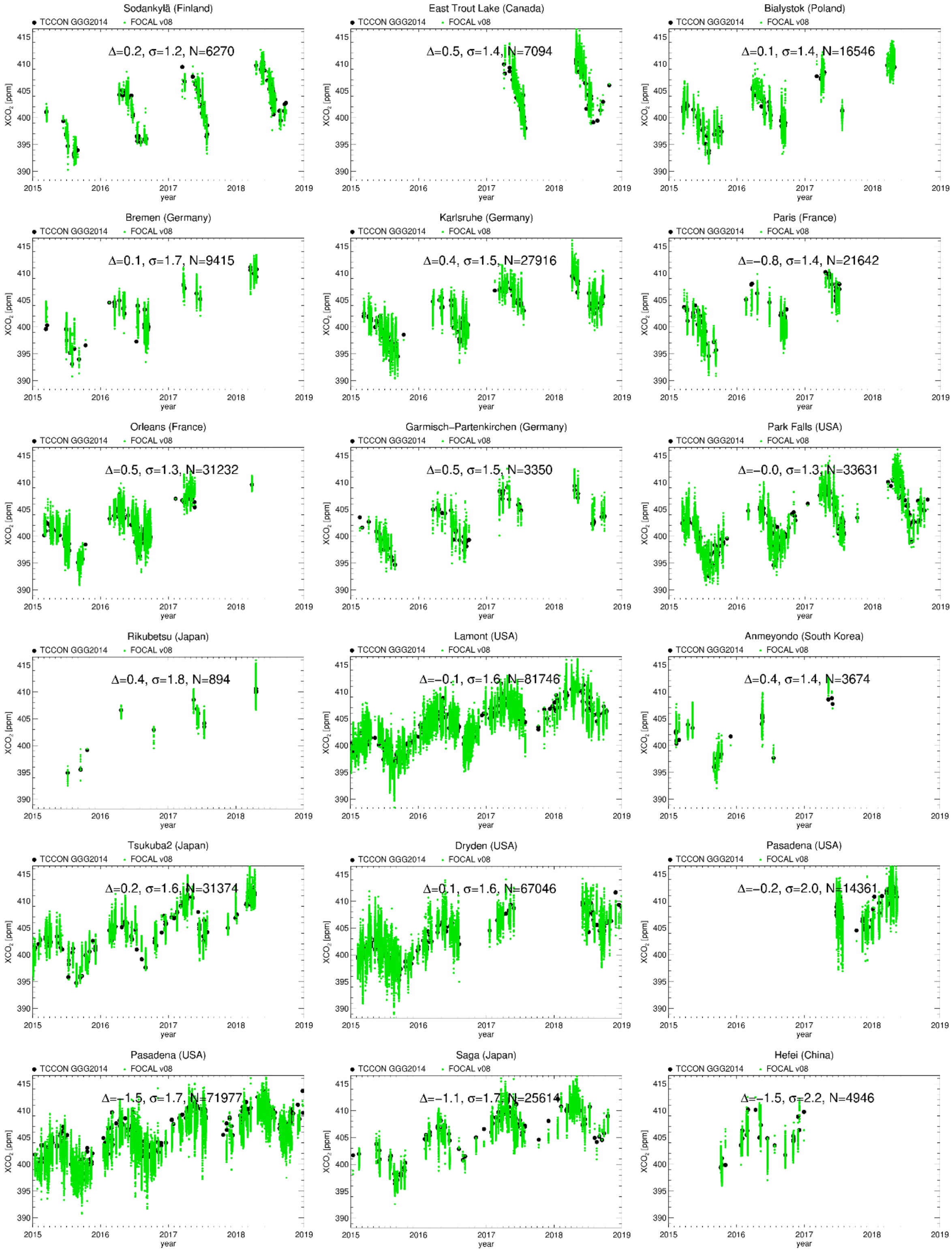
Sodankylä (Finland)
Δ=0.2, σ=1.2, N=6270
East Trout Lake (Canada)
Δ=0.5, σ=1.4, N=7094
Bialystok (Poland)
Δ=0.1, σ=1.4, N=16546
Bremen (Germany)
Δ=0.1, σ=1.7, N=9415
Karlsruhe (Germany)
Δ=0.4, σ=1.5, N=27916
Paris (France)
Δ=−0.8, σ=1.4, N=21642
Orleans (France)
Δ=0.5, σ=1.3, N=31232
Garmisch−Partenkirchen (Germany)
Δ=0.5, σ=1.5, N=3350
Park Falls (USA)
Δ=−0.0, σ=1.3, N=33631
Rikubetsu (Japan)
Δ=0.4, σ=1.8, N=894
Lamont (USA)
Δ=−0.1, σ=1.6, N=81746
Anmeyondo (South Korea)
Δ=0.4, σ=1.4, N=3674
Tsukuba2 (Japan)
Δ=0.2, σ=1.6, N=31374
Dryden (USA)
Δ=0.1, σ=1.6, N=67046
Pasadena (USA)
Δ=−0.2, σ=2.0, N=14361
Pasadena (USA)
Δ=−1.5, σ=1.7, N=71977
Saga (Japan)
Δ=−1.1, σ=1.7, N=25614
Hefei (China)
Δ=−1.5, σ=2.2, N=4946
TCCON GGG2014
FOCAL v08
XCO2 [ppm]
year

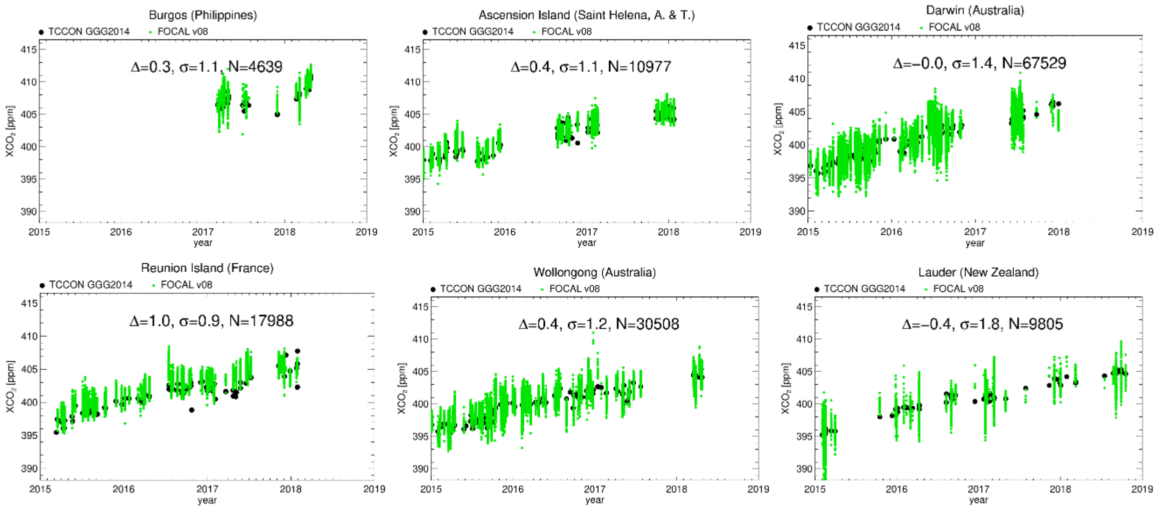

Figure 20: Validation of single soundings of FOCAL (green) with co-located TCCON measurements (black) at all TCCON sites with more than 250 co-locations and covering a time period of at least one year. Numbers in the figures: Δ = station bias, i.e., average of the difference; σ = single measurement precision, i.e., standard deviation of the difference; N = number of co-locations.

Due to the relatively large uncertainty, we decided to compute not the maximum minus minimum as a measure for the year-to-year stability because this quantity can be expected to increase with length of the time series simply due to statistics. Therefore, we estimate the year-to-year stability by randomly selecting pairs of dates with a time difference of at least 365 days. For each selection we computed the difference modified by a random component corresponding to the estimated uncertainty. From 1000 of such pairs we compute the standard deviation as estimate for the year-to-year stability. We repeat this experiment 1000 times and compute the average (0.21 ppm) and standard deviation (0.01 ppm).

From this, we conclude that the year-to-year stability is 0.21 ppm/a (**Figure 21**).

Table 15: Validation statistics for all TCCON sites with more than 250 co-locations and covering a time period of at least one year with number of co-locations (#), single measurement precision (σ), station bias (Δ), seasonal bias (s) and linear drift (d). The last row contains the overall statistics. In this row σ represents the (quadratic) average single measurement precision, Δ the station-to-station bias (i.e., the standard deviation of the station biases), s the average seasonal bias, and d the average drift plus minus its standard deviation.

Station	#	σ [ppm]	Δ [ppm]	s [ppm]	d [ppm/a]
Sodankylä	6270	1.16	0.23	0.24	-0.08
East Trout Lake	7094	1.44	0.46	0.64	0.46
Bialystok	16546	1.38	0.14	0.12	0.00
Bremen	9415	1.71	0.13	0.40	-0.34
Karlsruhe	27916	1.49	0.39	0.70	0.16
Paris	21642	1.36	-0.80	0.48	-0.08
Orleans	31232	1.31	0.50	0.20	0.24
Garmisch-P.	3350	1.53	0.52	0.52	0.23
Park Falls	33631	1.34	-0.04	0.56	0.15
Rikubetsu	894	1.78	0.45	0.58	0.76
Lamont	81746	1.62	-0.13	0.18	-0.16
Anmeyondo	3674	1.37	0.39	0.29	-0.25
Tsukuba	31374	1.60	0.20	0.19	0.25
Dryden	67046	1.59	0.14	0.39	-0.04
Pasadena	14361	2.01	-0.23	1.01	-3.19
Pasadena	71977	1.68	-1.46	0.22	-0.12
Saga	25614	1.66	-1.07	0.18	0.14
Heifei	4946	2.21	-1.51	0.25	1.01
Burgos	4639	1.10	0.31	0.15	0.60
Ascension Island	10977	1.11	0.40	0.23	0.17
Darwin	67529	1.41	-0.01	0.24	-0.06
Reunion Island	17988	0.94	1.04	0.30	0.00
Wollongong	30508	1.24	0.37	0.31	-0.16
Lauder	9805	1.84	-0.40	0.81	0.35
Total	**600174**	**1.52**	**0.64**	**0.38**	**0.00±0.75**

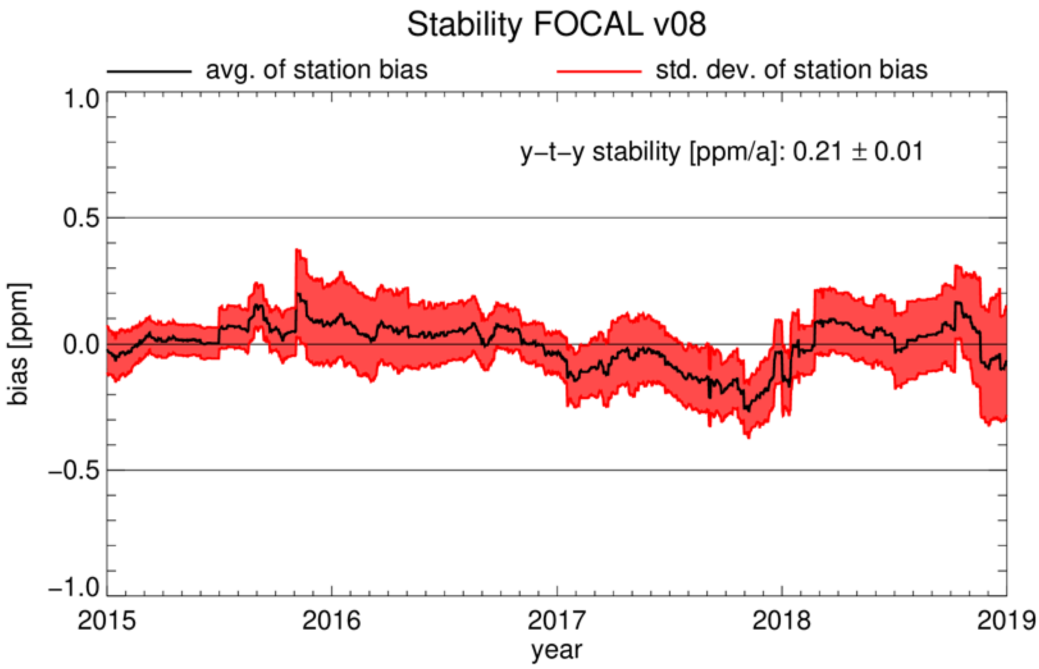

Figure 21: Stability analyses for product CO2_OC2_FOCA. The black curve shows the average station bias and the red curves its uncertainty represented by the station-to-station standard deviation and error propagation from single sounding measurement noise.

XCO_2 uncertainty

Especially for the application of flux inversion, reliable information on the uncertainty of each individual sounding is necessary. For this purpose, we analyzed the same validation dataset of co-located FOCAL and TCCON measurements as before.

For each co-location used for the shown TCCON validation, we have a residual ε of the bias model ΔX. From this residual, we computed our best estimate for the stochastic uncertainty (precision) as it does not include the analyzed systematic biases (trend, seasonal cycle, station-to-station).

For each ε, we have a corresponding uncertainty reported by FOCAL's optimal estimation retrieval. We pooled the entire data set of about 600000 co-locations into 20 bins with increasing reported uncertainty in a way that each bin included the same number of co-locations (about 30000). In each bin, we computed the (quadratic) average reported uncertainty and the standard deviation of the residual ε (true precision).

Figure 22 shows that both quantities are connected by a more or less linear relationship, except for an outlier in the bin of the largest reported uncertainties. The reported uncertainty is mainly driven by the instrumental noise which is in turn driven by the radiance so that the darkest scenes usually have the largest reported uncertainties. This means, especially the bins including the largest (or smallest) reported uncertainties may be dominated by an individual validation site with especially dark (or bright) albedo, while the other bins usually consist of data from a lager mixture of TCCON sites.

The linear fit shown in **Figure 22** shows that FOCAL's reported uncertainties has a positive correlation with the true precision but it shows also that FOCAL's reported uncertainty is somewhat to optimistic. However it shall be noted that the residual ε does not only include instrumental noise but also pseudo noise from representation errors.

In summary, we suggest that users who are interested in more realistic uncertainty estimates, shall apply the following error parameterization derived from the linear fit shown in **Figure 22**.

$$\sigma_{\mathrm{corrected}}^{\mathrm{XCO_2}} = \sigma_{\mathrm{v08}}^{\mathrm{XCO_2}} \cdot 1.128 + 0.128\mathrm{ppm}$$

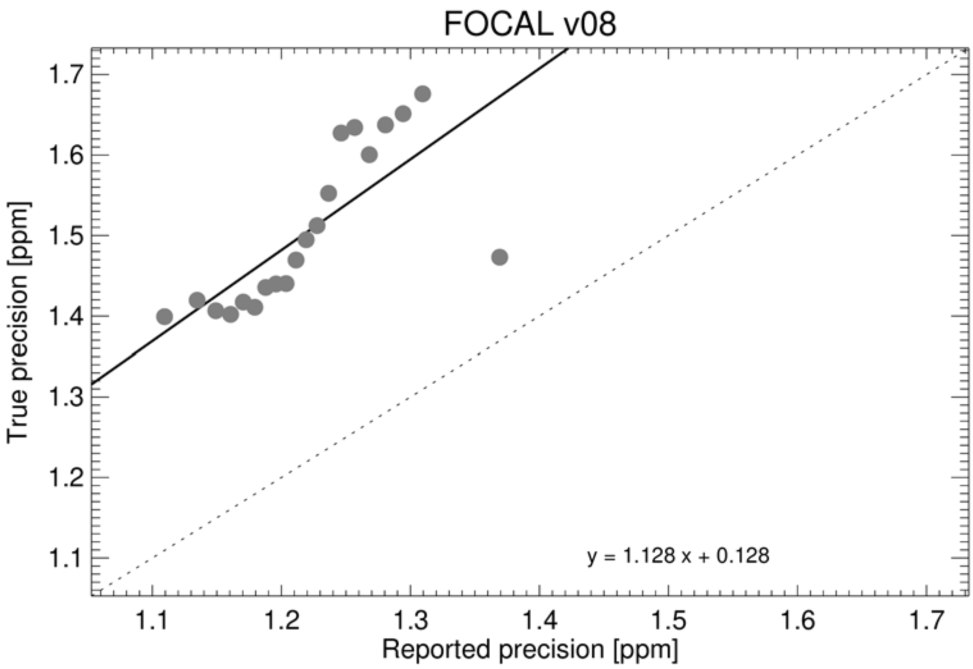

Figure 22: Reported uncertainty of FOCAL's optimal estimation retrieval vs. true precision computed from the residual $\boldsymbol{\varepsilon}$ of the bias model.

5.1.1.4 Summary

Table 13 presents an overview of the estimated data quality as obtained from comparisons with TCCON ground-based reference observations.

Table 16: Summary validation of product CO2_OC2_FOCA by the independent validation team using TCCON ground-based reference data.

Product Quality Summary Table for Product: CO2_OC2_FOCA Level: 2, Version: v08, Time period covered: 01/2015 – 12/2018 Assessment: Data Provider (DP)			
Parameter [unit]	**Achieved performance**	**Requirement**	**Comments**
Single measurement precision (1-sigma) in [ppm]	1.52	< 8 (T) < 3 (B) < 1 (G)	Computed as standard deviation of the difference to TCCON
Uncertainty ratio [-]: Ratio reported uncertainty to standard deviation of satellite-TCCON difference	0.81	-	No requirement but value close to unity expected for a high quality data product with reliable reported uncertainty.
Mean bias (global offset) [ppm]	-0.31	-	No requirement but value close to zero expected for a high quality data product.
Accuracy: Relative systematic error [ppm]	Spatial: 0.64 Spatio-temporal: 0.74	< 0.5	Spatial: Computed as standard deviation of the biases at the various TCCON sites. Spatio-temporal: As "Spatial" but also considering seasonal biases.
Stability: Drift [ppm/year]	0.00±0.75 (1-sigma)	< 0.5	Linear drift

5.1.2 Validation and intercomparison results for product CO2_TAN_OCFP

The UoL core CO_2 ECV product (CO2_TAN_OCFP v1) is retrieved from calibrated TanSat SWIR/NIR spectra using the UoL full-physics retrieval algorithm **/Boesch et al., 2011/**. The TanSat L1 spectra are retrieved for all TCCON overpasses for the time period March 2017 to May 2018 and are evaluated against rigorously validated ground based TCCON values.

5.1.2.1 Detailed results

To assess the quality of CO2_TAN_OCFP v1 observations against TCCON, OCFP (TanSat) soundings are matched to TCCON observations spatially and temporally. OCFP (TanSat) points are co-located with TCCON sites based on a quadrate latitude and longitude region around each TCCON site (in ±3º latitude/longitude box). Matching OCFP soundings with TCCON sites for time is a comparatively simple operation, selecting only those TCCON values whose observation time falls within ±1 hour of each TanSat sounding time. The average is taken of all TCCON points fitting these criteria for each OCFP sounding to provide the TCCON value against which to compare.

The co-location procedure matches 113,120 points for the CO2_TAN_OCFP v1 product. The comparions for each TCCON site is shown in **Figure 23** and the statics (mean bias, standard deviation and Pearson correlation coefficient R) for each site is given in **Table 14**. The bias per site varies between -1.40 ppm and 1.57 ppm with a standard deviation of the per-site bias of 0.84 ppm. It is important to highlight that the number of data points and the temporal coverage varies greatly between sites.

The overall correlation between the TanSat and TCCON retrievals is given in **Figure 24**. We find a small mean overall bias of 0.19 ppm and an all-site Pearson correlation coefficient of 0.82 which details a good match of OCFP and TCCON pairs. The all-site RMSE (mean of the standard deviation per site) of Δ (TCCON- OCFP) is 1.78 ppm.

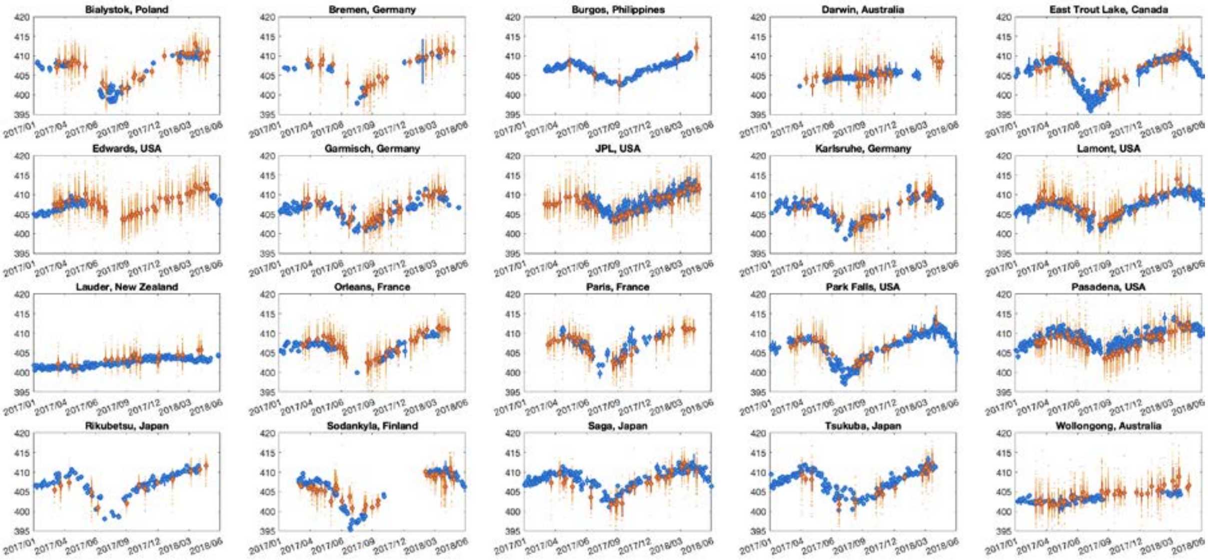

Figure 23: TanSat XCO_2 (product CO2_TAN_OCFP v1) observations plotted with their corresponding paired TCCON mean (blue) for the overpass. Overview statistics for each site reference to **Table 14**.

Table 17: Overview of the estimated data quality as obtained from comparisons with TCCON ground-based reference observations per site. The bottom row details statistics for all sites, with all co-located points used for calculations. XCO_2 units is in ppm. The overall mean Δ and σΔ is calculated by averaging of site values and R is calculated by all individual measurements.

Site	Mean Δ	σΔ	*R*	n obs.
Bialystok, Poland	-0.92	1.68	0.65	3,292
Bremen, Germany	0.25	1.20	0.25	1,610
Burgos, Philippines	-0.08	2.22	0.32	310
Darwin, Australia	-0.64	2.05	-0.33	5,534
East Trout Lake, Canada	-0.17	1.26	0.90	11,923
Edwards, USA	-1.40	1.96	0.55	2,763
Garmisch, Germany	-0.32	1.67	0.67	3,704
JPL, USA	1.17	2.07	0.81	15,209
Karlsruhe, Germany	-0.29	1.62	0.84	3,089
Lamont, USA	-0.35	1.35	0.86	18,274
Lauder, New Zealand	-1.31	1.88	0.72	2,999
Orléans, France	-0.66	1.46	0.18	2,243
Paris, France	-0.08	1.40	0.76	1,503
Park Falls, USA	-0.35	1.45	0.89	13,231
Pasadena, USA	1.57	2.47	0.65	12,807
Rikubetsu, Japan	0.54	1.27	0.84	1,473
Sodankylä Finland	-1.18	2.19	0.93	6,482
Saga, Japan	0.69	1.99	0.77	4,033
Tsukuba, Japan	0.94	2.46	0.79	866
Wollongong, Australia	-1.15	1.93	0.73	1,775
Overall	0.19	1.78	0.82	113,120

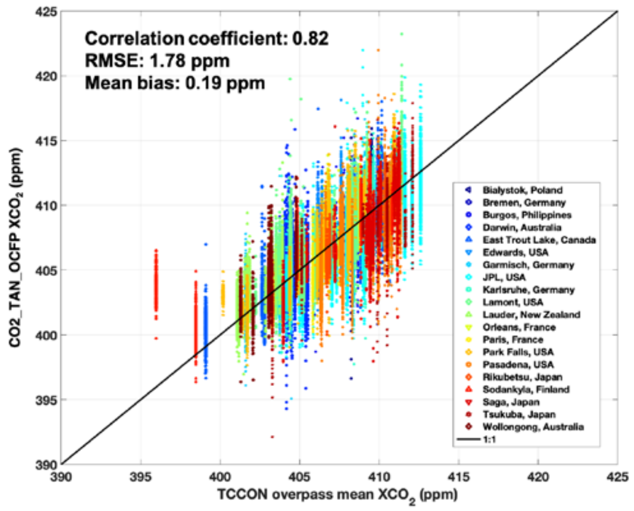

Figure 24: Correlation plot between all 113,120 co-located CO2_TAN_OCFP and TCCON XCO_2 pairs coloured by site.

The random error is assessed by comparing the overpass-mean reported uncertainty for an overapss over a TCCON site to the standard deviation of the TCCON–OCFP pairs for each overpass. **Figure 25** shows that the reported uncertainties are between 0.78 ppm (Lamont, U.S.A.) and 4.34 ppm (East Trout Lake, Canada). There is a relatively large spread of the data points with some clear outliers where the observed scatter is largely overestimated. We find that these overestimated errors are correlated with very low surface albedo of the CO_2 band and subsequently low information content for CO_2 so that the retrieved results remain close to the a priori values. The slope between the observed scatter between TanSat and TCCON retrievals and the reported uncertainties is 0.96.

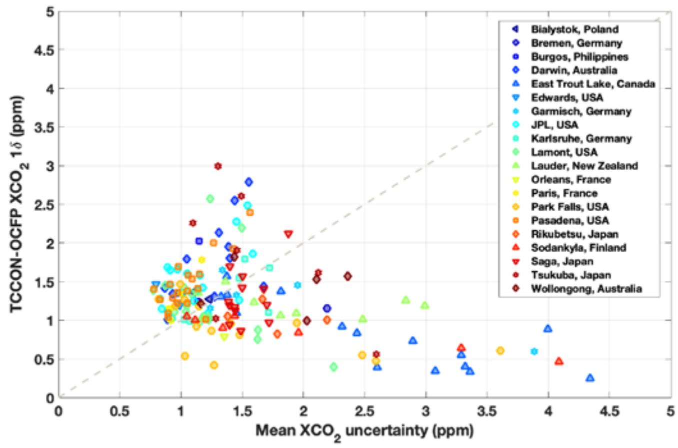

Figure 25: Correlation plot of the TCCON–OCFP ∆ standard deviation per TCCON overpass and the reported overpass-mean a posteriori retrieval error for different TCCON sites.

5.1.2.2 Summary

The result of the validation of the CO2_TAN_OCFP v1.0 dataset is given in **Table 15** and compared to the requirement. The mean estimate of the single-measurement precision is 1.78 ppm which exceeds the goal requirement but is within the baseline requirement of 3 ppm. The reported uncertainties agree in average with the observed scatter of the data when compared to TCCON. The mean, global bias of the TanSat XCO_2 retrieval is 0.19 ppm with a relative accuracy of 0.84 ppm which is slightly larger than the requirement of 0.5 ppm. We have not assessed the spatio-temporal bias or the drift due to the short time period covered by the CO2_TAN_OCFP dataset.

Table 18: Summary validation of product CO2_TAN_OCFP by the data provider using TCCON ground-based reference data.

Product Quality Summary Table for Product: CO2_TAN_OCFP Level: 2, Version: v1, Time period covered: 3.2017 – 5.2018 Assessment: Data Provider (DP)			
Parameter [unit]	**Achieved performance**	**Requirement**	**Comments**
Single measurement precision (1-sigma) in [ppm]	1.78	< 8 (T) < 3 (B) < 1 (G)	Computed as standard deviation of the difference to TCCON
Uncertainty ratio [-]: Ratio reported uncertainty to standard deviation of satellite-TCCON difference	0.96	-	No requirement but value close to unity expected for a high quality data product with reliable reported uncertainty.
Mean bias (global offset) [ppm]	0.19	-	No requirement but value close to zero expected for a high quality data product.
Accuracy: Relative systematic error [ppm]	Spatial: 0.84 Spatio-temporal: Not evaluated	< 0.5	Spatial: Computed as standard deviation of the biases at the various TCCON sites. Spatio-temporal: As "Spatial" but also considering seasonal biases.
Stability: Drift [ppm/year]	Not evaluated	< 0.5	Linear drift

5.1.3 Validation and intercomparison results for product CO2_GO2_SRFP

First retrieval results for this product will be generated in the second year of this project. Therefore, no validation / intercomparison results are shown in this first version of this document.

5.1.4 Validation and intercomparison results for product CH4_S5P_WFMD

Validation results for XCH_4 retrieved from TROPOMI with the WFMDv1.2 algorithm are summarised in this section. The validation data set is the GGG2014 collection of the Total Carbon Column Observing Network (TCCON) (available from https://tccondata.org/). To ensure comparability, all TCCON sites use similar instrumentation (Bruker IFS 125HR) and a common retrieval algorithm. The TCCON data are tied to the WMO trace gas scale using airborne in situ measurements applying individual scaling factors for each species. The estimated TCCON accuracy (1σ) is about 3.5 ppb for XCH_4. From the validation with TCCON data at 21 TCCON sites, realistic error estimates of the satellite data are provided. The validation results are largely adopted from **/Schneising et al., 2019/.**

To compare the satellite data with TCCON quantitatively, it has to be taken into account that the sensitivities of the instruments differ from each other and that individual apriori profiles are used to determine the best estimate of the true atmospheric state, respectively. The first step is to correct for the apriori contribution to the smoothing equation by adjusting the measurements for a common apriori. Here we use the TCCON prior as the common apriori profile for all measurements:

$$\hat{c}_{adj} = \hat{c} + \frac{1}{m_0}\sum_l m_l\,(1 - A_l)(x^l_{a,T} - x^l_a)$$

In this equation, $\hat{c}$ represents the originally retrieved TROPOMI column-averaged dry air mole fraction, l is the index of the vertical layer, A_l the corresponding column averaging kernel of the TROPOMI algorithm, $\boldsymbol{x}_a$ and $\boldsymbol{x}_{a,T}$ the TROPOMI and TCCON apriori dry air mole fraction profiles. m_l is the mass of dry air determined from the dry air pressure difference between the upper and lower boundary of layer l and $m_0 = \sum_l m_l$ is the total mass of dry air. To minimise the smoothing error introduced by the averaging kernels we do not compare $\hat{c}_{adj}$ directly with the retrieved TCCON mole fractions $\hat{c}_T$ but rather with the adjusted expression

$$\hat{c}_{T,adj} = c_{a,T} + \left(\frac{\hat{c}_T}{c_{a,T}} - 1\right)\frac{1}{m_0}\sum_l m_l A_l x^l_{a,T}$$

Thereby, $c_{a,T}$ represents the TCCON apriori column-averaged dry air mole fraction associated with the apriori profile $\boldsymbol{x}_{a,T}$.

5.1.4.1 Detailed results

For the comparison a set of collocation criteria has been specified. The representativity is maximised by as strict as possible criteria while concurrently ensuring sufficient data for a sound and stable comparison. This trade-off is resolved by the following selection. The spatial collocation criterion requires the satellite measurements to lie within a radius of 100 km around the TCCON site and that the altitude difference is smaller than 250 m. The temporal collocation criterion is set to ±2 hours. For each satellite measurement within the collocation radius, all TCCON data meeting the temporal collocation criterion are averaged to obtain a unique satellite-TCCON data pair. This approach is consistent with the well-established methods used in previous GHG-CCI PVIRs by the independent validation team and by the data providers.

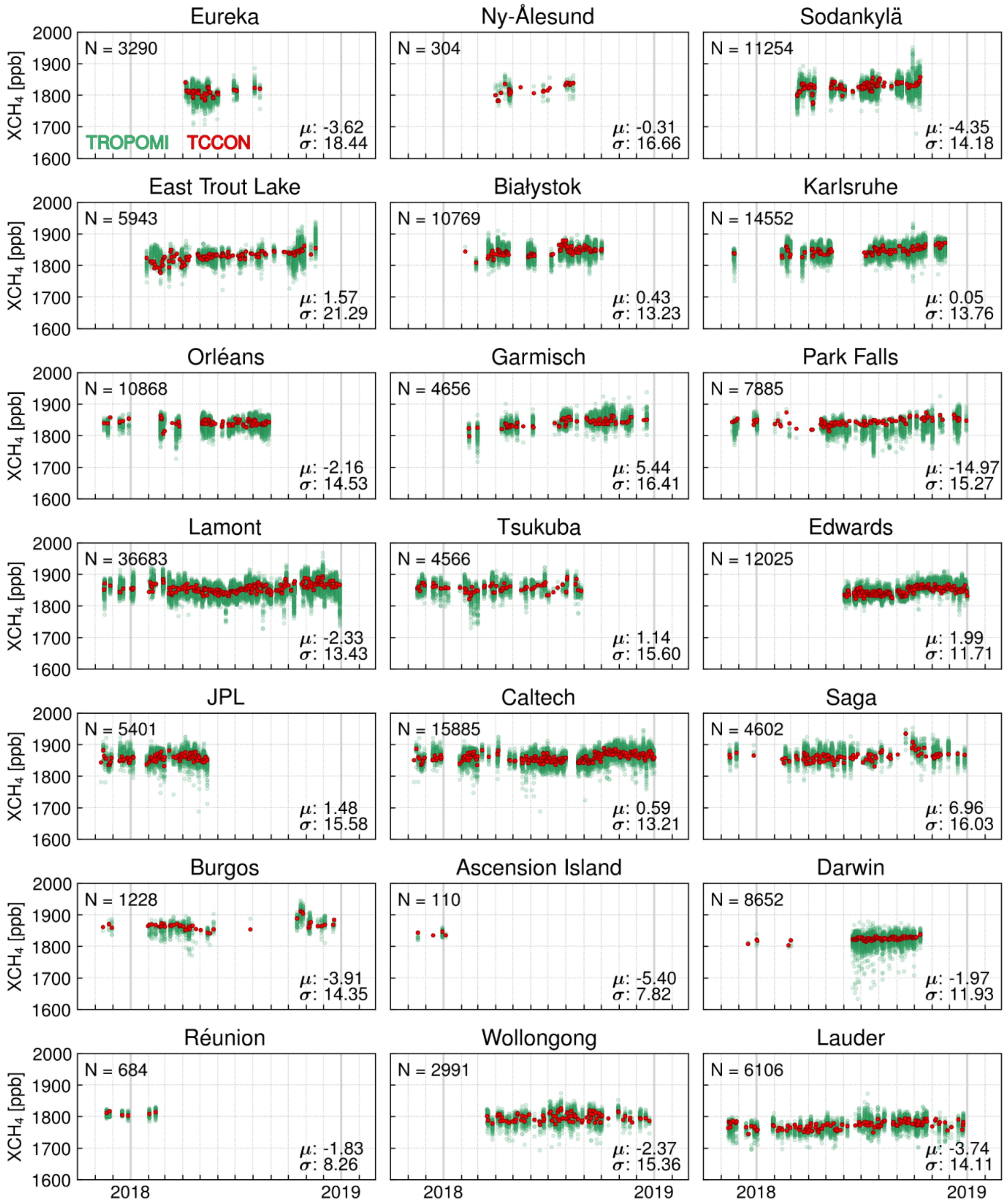

Figure 26: Comparison of the TROPOMI/WFMD v1.2 XCH_4 time series (green) with ground-based measurements from the TCCON (red). For each site, ***N*** is the number of collocations, $\boldsymbol{\mu}$ corresponds to the mean bias and $\boldsymbol{\sigma}$ to the scatter of the satellite data relative to TCCON in ppb.

However, please note that the independent validation of the validation team now uses a completely different approach ignoring most of the satellite measurements and the effects of the averaging kernels. We stick to our tried and tested method utilising all satellite data around the TCCON sites, because otherwise a robust and stable estimation of the figures of merit would appear questionable.

The validation results are summarised in **Figure 26** including the mean bias μ and the scatter σ relative to TCCON for each site. As a consequence of the altitude representativity criterion, there are not enough collocations for a robust comparison at the mountain sites Zugspitze and Izaña. The parameter σ is estimated from Huber's Proposal-2 M-estimator, which is a well-established estimator of location and scale being robust against outliers of a normal distribution. This is an appropriate choice and preferred over the standard deviation, because one is interested in the actual single measurement precision without distortion of the results by a few outliers, which are rather attributed to systematic errors, e.g. due to residual clouds. As a consequence, outliers are fully included in the computation of the systematic error but get lower weight in the robust determination of the random error, which is interpreted as a measure of the repeatability of measurements.

It is also checked whether the respective site biases are sensitive to the selection of the spatial collocation radius, which is an indication of sources within the satellite collocation area with only marginal influence on the TCCON measurements itself. A considerable sensitivity was found for XCH_4 at Edwards. The collocation region intersects oil production areas in California's Central Valley (in contrast to Caltech and JPL, see **/Schneising et al., 2019/**) as well as the South Coast Air Basin (SoCAB), which has a well-known methane enhancement. As such nearby sources limit the representativity of affected satellite measurements, the collocation radius is reduced to 50 km for Edwards.

The results for the individual sites are condensed to the following parameters for the overall quality assessment of the satellite data: the global offset is defined as the mean of the local offsets at the individual sites, the random error is the global scatter of the differences to TCCON after subtraction of the respective regional biases, and the (spatial) systematic error is the standard deviation of the local offsets relative to TCCON at the individual sites as a measure of the station-to-station biases. For XCH_4 the global offset amounts to -1.30 ppb, the random error is 14.04 ppb (15.77 ppb when using the standard deviation instead of Huber's Proposal-2 M-estimator), and the (spatial) systematic error is given by 4.31 ppb. The seasonal systematic error is defined as the standard deviation of the four overall seasonal offsets (using all sites combined after subtraction of the respective local offsets) relative to TCCON and amounts to 0.57 ppb. The spatio-temporal systematic error (defined as the the root-sum-square of the spatial and seasonal systematic errors) amounts to 4.35 ppb, which is on the order of the estimated (station-to-station) accuracy of the TCCON of about 3.5 ppb.

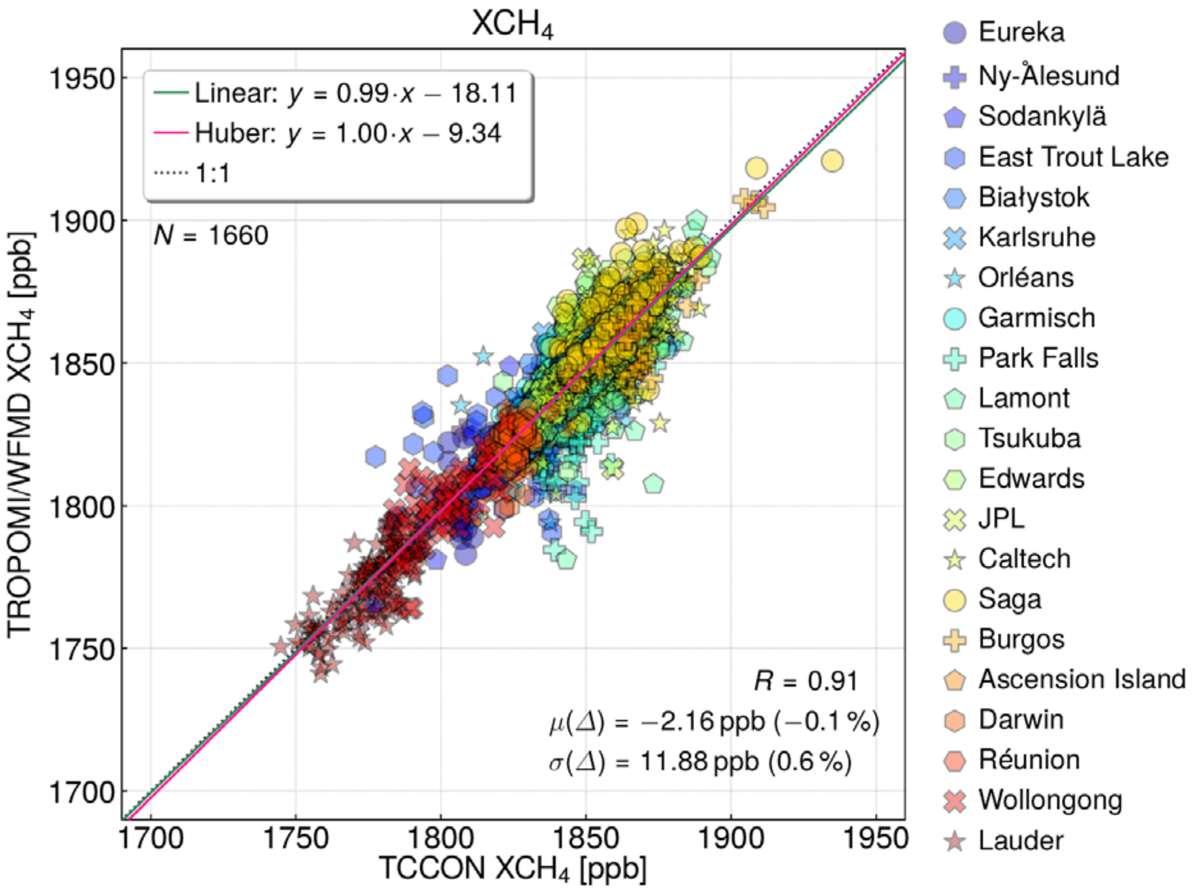

Figure 27: Comparison of the TROPOMI/WFMD data to the TCCON based on daily means. Specified are the linear regression results and the correlation of the data sets, as well as the mean and standard deviation of the difference. To analyse the impact of outliers, the regression is also performed for the Huber linear regression model, which is robust to outliers.

Long-term drift stability, and year-to-year stability are not determined at this juncture because the temporal coverage of the analysed time series is too short for a sound and stable estimation of these figures of merit.

To further analyse how well the real temporal and spatial variations are captured by the TROPOMI data, **Figure 27** shows a comparison to TCCON based on daily means for days with more than three collocations. The obvious linear relationship with a high correlation of $R = 0.91$ underlines the typical good agreement of the satellite and validation data.

There are a few outliers where the satellite values are considerably lower than the TCCON values. These occasional instances are not site specific and can probably be ascribed to days with residual or partial cloud cover interfering with the satellite retrievals. Outliers with higher values compared to TCCON are more rare and dominated by a handful of collocations at East Trout Lake. This exceptional lack of agreement occurs on four days in the time period February 10-21 as well as on March 29 and may be attributable to Arctic polar vortex air above East Trout Lake potentially causing the following related issues: associated fronts of different air masses may complicate the identification of collocations near the vortex edge and/or the stratospheric part of the methane profile may be largely affected by the polar vortex leading to a considerable deviation from the assumed apriori profile shapes. It is verified that the impact of outliers on the regression is marginal by repeating the fit with the Huber linear regression model, which is robust to outliers and provides similar results to the standard linear regression here.

The reported uncertainty of TROPOMI/WFMD v1.2 XCH4 is estimated during the inversion procedure via error propagation from the uncorrelated spectral measurement errors given in the TROPOMI Level 1 files. The (unknown) pseudo-noise component determined by specific atmospheric parameters or instrumental features is not considered and thus the reported uncertainty σ is typically underestimating the actual uncertainty. To obtain a more realistic uncertainty estimate $\hat{\sigma}$, an error parameterisation based on a comparison of the reported uncertainty and measured scatter relative to the TCCON for different sites and seasons was introduced in the End-to-End ECV Uncertainty Budget (E3UB) and recommended to be applied in the Product User Guide (PUG) :

$$\hat{\sigma} = \sigma + 9\, ppb$$

After application of this uncertainty correction, the uncertainty ratio (reported uncertainty to measured scatter) improves from 0.32 to 0.96.

5.1.4.2 Summary

In summary, the natural XCH_4 variations are well captured by the satellite data. We find a single measurement precision of the TROPOMI data of about 0.8%, while the station-to-station accuracy of the satellite data (0.2%) is comparable to the TCCON.

The single measurement precision is below the breakthrough requirement and the uncertainty ratio is close to 1 after applying the uncertainty correction recommended in the Product User Guide. The accuracy also complies with the requirements and the mean bias is close to zero. The stability was not assessed because the temporal coverage of the analysed time series is too short for a sound and stable estimation. **Table 16** presents an overview of the estimated data quality as obtained from comparisons with TCCON ground-based reference observations.

Table 19: Summary validation of product CH4_S5P_WFMD by the data provider using TCCON ground-based reference data.

Product Quality Summary Table for Product: CH4_S5P_WFMD Level: 2, Version: v1.2, Time period covered: 11.2017 – 12.2018 Assessment: Data Provider (DP)			
Parameter [unit]	**Achieved performance**	**Requirement**	**Comments**
Single measurement precision (1-sigma) in [ppb]	14.04	< 34 (T) < 17 (B) < 9 (G)	Computed as standard deviation of the difference to TCCON
Uncertainty ratio [-]: Ratio reported uncertainty to standard deviation of satellite-TCCON difference	0.96 After uncertainty correction recommended in the Product User Guide	-	No requirement but value close to unity expected for a high quality data product with reliable reported uncertainty.
Mean bias (global offset) [ppb]	-1.30	-	No requirement but value close to zero expected for a high quality data product.
Accuracy: Relative systematic error [ppb]	Spatial: 4.31 Spatio-temporal: 4.35	< 10	Spatial: Computed as standard deviation of the biases at the various TCCON sites. Spatio-temporal: As "Spatial" but also considering seasonal biases.
Stability: Drift [ppb/year]	n/a (1-sigma)	< 3	Linear drift

5.1.5 Validation and intercomparison results for product CH4_GO2_SRFP

First retrieval results for this product will be generated in the second year of this project. Therefore, no validation / intercomparison results are shown in this first version of this document.

5.1.6 Validation and intercomparison results for product CH4_GO2_SRPR

First retrieval results for this product will be generated in the second year of this project. Therefore, no validation / intercomparison results are shown in this first version of this document.

6 References

/Aben et al., 2019/ Aben, I., L. Wu, O. Hasekamp, M. Buchwitz, M. Reuter, O. Schneising, H. Boesch, D. Yang, ESA Climate Change Initiative “Plus” (CCI+) System Specification Document (SSD) for the Essential Climate Variable (ECV) Greenhouse Gases (GHG): XCO_2 and/or XCH_4 from OCO-2, TanSat, Sentinel-5-Precursor and GOSAT-2, Version 1.0, 26-August-2019, pp. 33, 2019.

/Ackermann et al., 2010/ Ackerman, S.; Frey, R.; Strabala, K.; Liu, Y.; Gumley, L.; Baum, B.; Menzel, P. Discriminating Clear-Sky from Cloud with MODIS—Algorithm Theoretical Basis Document (MOD35); Version 6.1; Cooperative Institute for Meteorological Satellite Studies, University ofWisconsin—Madison: Madison, WI, USA, 2010.

/ATBDv1 FOCAL, 2019/ Reuter et al.: Algorithm Theoretical Basis Document Version 1 (ATBDv1) - Retrieval of XCO_2 from the OCO-2 satellite using the Fast Atmospheric Trace Gas Retrieval (FOCAL), ESA GHG-CCI project, 2019.

/Boesch et al., 2011/ Boesch, H., Baker, D., Connor, B., Crisp, D., and Miller, C.: Global characterization of CO_2 column retrievals from shortwave-infrared satellite observations of the Orbiting Carbon Observatory-2 mission, Remote Sens., 3, 270–304, doi:10.3390/rs3020270, 2011.

/Butz et al., 2009/ Butz, André, Otto P. Hasekamp, Christian Frankenberg, and Ilse Aben, "Retrievals of atmospheric CO_2 from simulated space-borne measurements of backscattered near-infrared sunlight: accounting for aerosol effects," Appl. Opt. 48, 3322-3336 (2009)

/Butz et al., 2010/ Butz, André, Otto P. Hasekamp, Christian Frankenberg, Jerome Vidot, and Ilse Aben, ",CH4 retrievals from space-based solar backscatter measurements: Performance evaluation against simulated aerosol and cirrus loaded scenes" , J. Geophys. Res., 115, 24,302, doi:10.1029/2010JD014514, 2010.

/Butz et al., 2011/ Butz, A., S. Guerlet, O. Hasekamp, et al., Toward accurate CO_2 and CH_4 observations from GOSAT, Geophys. Res. Lett., Geophys. Res. Lett., doi:10.1029/2011GL047888, 2011.

/CECRv3 BESD, 2017/ M. Reuter, O. Schneising, M. Buchwitz, J. Heymann: Comprehensive Error Characterisation Report: BESD full-physics retrieval algorithm for XCO_2 for the Essential Climate Variable (ECV) Greenhouse Gases (GHG), ESA GHG-CCI project, 2017.

/Eldering et al., 2015/ Eldering, A.; Pollock, R.; Lee, R.; Rosenberg, R.; Oyafuso, F.; Crisp, D.; Chapsky, L.; Granat, R. Orbiting Carbon Observatory-2 (OCO-2) - LEVEL 1B - Algorithm Theoretical Basis; Version 1.2 Rev 1; National Aeronautics and Space Administration, Jet Propulsion Laboratory, California Institute of Technology: Pasadena, CA, USA, 2015

/Frankenberg et al., 2005/ Frankenberg, C., Meirink, J.F., van Weele, M., Platt, U., Wagner, T. (2005), Assessing methane emissions from global space-borne obseravtions, Science, ., doi:10.1126/science.1106644

/Frankenberg et al., 2011/ Frankenberg, C., Aben, I., Bergamaschi, P., et al. (2011), Global column-averaged methane mixing ratios from 2003 to 2009 as derived from SCIAMACHY: Trends and variability, J. Geophys. Res., doi:10.1029/2010JD014849.

/GCOS-154/ Global Climate Observing System (GCOS), SYSTEMATIC OBSERVATION REQUIREMENTS FOR SATELLITE-BASED PRODUCTS FOR CLIMATE, Supplemental details to the satellite-based component of the "Implementation Plan for the Global Observing System for Climate in Support of the UNFCCC (2010 update)", Prepared by World Meteorological Organization (WMO), Intergovernmental Oceanographic Commission, United Nations Environment Programme (UNEP), International Council for Science, Doc.: GCOS 154, link: http://cci.esa.int/sites/default/files/gcos-154.pdf, 2011.

/GCOS-195/ Status of the Global Observing System for Climate. GCOS-195. Link: https://library.wmo.int/pmb_ged/gcos_195_en.pdf, 2015.

/GCOS-200/ The Global Observing System for Climate: Implementation Needs, GCOS 2016 Implementation Plan, World Meteorological Organization (WMO), GCOS-200 (GOOS-214), pp. 325, link: https://library.wmo.int/opac/doc_num.php?explnum_id=3417, 2016.

/HITRAN2016/ Gordon et al., The HITRAN2016 molecular spectroscopic database, J. Quant. Spectrosc. Radiat. Transfer, 203, 3-69, 2017.

/Kuruz, 1994/ Kurucz, H.L. The Solar Spectrum: Atlases and Line Identifications, Workshop on Laboratory and Astronomical High Resolution Spectra. Astronomical Society of the Pacific Conference Series. In Proceedings of the ASP Conference, Brussels, Belgium, 29 August–2 September 1994; pp. 17–31

/O'Dell et al., 2012/ O'Dell, C.W.; Connor, B.; Bösch, H.; O'Brien, D.; Frankenberg, C.; Castano, R.; Christi, M.; Eldering, D.; Fisher, B.; Gunson, M.; et al. The ACOS CO_2 retrieval algorithm - Part 1: Description and validation against synthetic observations. Atmos. Meas. Tech. 2012, 5, 99–121

/Parker et al., 2011/ Parker, R., Boesch, H, Cogan, A., et al. (2011), Methane Observations from the Greenhouse gases Observing SATellite: Comparison to ground-based TCCON data and Model Calculations, Geophys. Res. Lett., doi:10.1029/2011GL047871.

/PUGS, 2019/ Buchwitz, M., Aben, I., J., Armante, R., Boesch, H., Crevoisier, C., Di Noia, A., Hasekamp, O. P., Reuter, M., Schneising-Weigel, O., Wu, L.., Product User Guide and Specification (PUGS) – Main document for Greenhouse Gas (GHG: CO_2 & CH_4) data set CDR 3 (2003-2018), C3S project C3S_312b_Lot2_DLR, v3.1, 97 pages, https://www.iup.uni-bremen.de/carbon_ghg/docs/C3S/CDR3_2003-2018/PUGS/C3S_D312b_Lot2.3.2.3-v1.0_PUGS-GHG_MAIN_v3.1.pdf, 2019.

/PVIRv5, 2017/ Product Validation and Intercomparison Report" (PVIR), ESA Climate Change Initiative (CCI) GHG-CCI project, Version 5, 9 Feb 2017, 2017.

/Reuter et al., 2011/ Reuter, M., Bovensmann, H., Buchwitz, M., Burrows, J. P., Connor, B. J., Deutscher, N. M., Griffith, D.W. T., Heymann, J., Keppel-Aleks, G., Messerschmidt, J., and et al.: Retrieval of atmospheric CO_2 with enhanced accuracy and precision from SCIAMACHY: Validation with FTS measurements and comparison with model results., Journal of Geophysical Research, 116, doi:10.1029/2010JD015047, URL http://dx.doi.org/10.1029/2010JD015047, 2011

/Reuter et al., 2013/ Reuter, M., H. Boesch, H. Bovensmann, A. Bril, M. Buchwitz, A. Butz, J. P. Burrows, C. W. O'Dell, S. Guerlet, O. Hasekamp, J. Heymann, N. Kikuchi, S. Oshchepkov, R. Parker, S. Pfeifer, O. Schneising, T. Yokota, and Y. Yoshida, A joint effort to deliver satellite retrieved atmospheric CO_2 concentrations for surface flux inversions: the ensemble median algorithm EMMA, Atmos. Chem. Phys., 13, 1771-1780, 2013.

/Reuter et al., 2017a/ M.Reuter, M.Buchwitz, O.Schneising, S.Noël, V.Rozanov, H.Bovensmann and J.P.Burrows: A Fast Atmospheric Trace Gas Retrieval for Hyperspectral Instruments Approximating Multiple Scattering - Part 1: Radiative Transfer and a Potential OCO-2 XCO_2 Retrieval Setup, Remote Sensing, 9(11), 1159; doi:10.3390/rs9111159, 2017.

/Reuter et al., 2017b/ M.Reuter, M.Buchwitz, O.Schneising, S.Noël, H.Bovensmann and J.P.Burrows: A Fast Atmospheric Trace Gas Retrieval for Hyperspectral Instruments Approximating Multiple Scattering - Part 2: Application to XCO_2 Retrievals from OCO-2, Remote Sensing, 9(11), 1102; doi:10.3390/rs9111102, 2017.

/Rodgers, 2000/ Rodgers, C. D.: Inverse Methods for Atmospheric Sounding: Theory and Practice, World Scientific Publishing, 2000.

/**Schepers et al., 2012/** Schepers, D., Guerlet, S., Butz, A., et al. (2012), Methane retrievals from Greenhouse Gases Observing Satellite (GOSAT) shortwave infrared measurements: Performance comparison of proxy and physics retrieval algorithms, *J. Geophys. Res.*, 117, D10307, doi:10.1029/2012JD017549.

/Schneising et al., 2011/ Schneising, O., Buchwitz, M., Reuter, M., et al., Long-term analysis of carbon dioxide and methane column-averaged mole fractions retrieved from SCIAMACHY, Atmos. Chem. Phys., 11, 2881-2892, 2011.

/Schneising et al., 2012/ Schneising, O., Bergamaschi, P., Bovensmann, H., et al, Atmospheric greenhouse gases retrieved from SCIAMACHY: comparison to ground-based FTS measurements and model results, Atmos. Chem. Phys., 12, 1527-1540, 2012.

/Schneising et al., 2019/ Schneising, O., Buchwitz, M., Reuter, M., Bovensmann, H., Burrows, J. P., Borsdorff, T., Deutscher, N. M., Feist, D. G., Griffith, D. W. T., Hase, F., Hermans, C., Iraci, L. T., Kivi, R., Landgraf, J., Morino, I., Notholt, J., Petri, C., Pollard, D. F., Roche, S., Shiomi, K., Strong, K., Sussmann, R., Velazco, V. A., Warneke, T., and Wunch, D.: A scientific algorithm to simultaneously retrieve carbon monoxide and methane from TROPOMI onboard Sentinel-5 Precursor, Atmos. Meas. Tech., 12, 6771-6802, https://doi.org/10.5194/amt-12-6771-2019, 2019.

/Stammes, 2002/ Stammes, P. OMI Algorithm Theoretical Basis Document, Volume III, Clouds, Aerosols, and Surface UV Irradiance (ATBD-OMI-03); Royal Netherlands Meteorological Institute (KNMI): De Bilt, The Netherlands, 2002

/Thompson et al., 2012/ Thompson, D.R.; Chris Benner, D.; Brown, L.R.; Crisp, D.; Malathy Devi, V.; Jiang, Y.; Natraj, V.; Oyafuso, F.; Sung, K.; Wunch, D.; et al. Atmospheric validation of high accuracy CO_2 absorption coefficients for the OCO-2 mission. J. Quant. Spectrosc. Radiat. Transf. 2012, 113, 2265–2276

/URDv2.1/ User Requirements Document (URD), ESA Climate Change Initiative (CCI) GHG-CCI project, Version 2.1, 38 pages, 19-Oct-2016, http://cci.esa.int/sites/default/files/URDv2.1_GHG-CCI_Final.pdf, 2016.

/Wunch et al., 2010/ Wunch, D., Toon, G. C., Wennberg, P. O., Wofsy, S. C., Stephens, B. B., Fischer, M. L., Uchino, O., Abshire, J. B., Bernath, P., Biraud, S. C., Blavier, J.-F. L., Boone, C., Bowman, K. P., Browell, E. V., Campos, T., Connor, B. J., Daube, B. C., Deutscher, N. M., Diao, M., Elkins, J. W., Gerbig, C., Gottlieb, E., Griffith, D. W. T., Hurst, D. F., Jiménez, R., Keppel-Aleks, G., Kort, E. A., Macatangay, R., Machida, T., Matsueda, H., Moore, F., Morino, I., Park, S., Robinson, J., Roehl, C. M., Sawa, Y., Sherlock, V., Sweeney, C., Tanaka, T., and Zondlo, M. A.: Calibration of the Total Carbon Column Observing Network using aircraft profile data, Atmospheric Measurement Techniques, 3, 1351–1362, doi:10.5194/amt-3-1351-2010, URL http://www.atmos-meas-tech.net/3/1351/2010/, 2010.

/Wunch et al., 2011/ Wunch, D., Toon, G. C., Blavier, J.-F. L., Washenfelder, R. A., Notholt, J., Connor, B. J., Griffith, D. W. T., Sherlock, V., and Wennberg, P. O.: The Total Carbon Column Observing Network (TCCON), Philosophical Transactions of the Royal Society of London, Series A: Mathematical, Physical and Engineering Sciences, 369, 2087–2112, doi:10.1098/rsta.2010.0240, 2011.

7 List of Acronyms and Abbreviations

Abbreviation	Meaning
AAI	Absorbing Aerosol Index
ACA	Additional Constraints Algorithm
AOD	Aerosol Optical Depth
AOT	Aerosol Optical Thickness
ATBD	Algorithm Theoretical Basis Document
BIRA-IASB	Royal Belgian Institute for Space Aeronomy
CCI	Climate Change Initiative
CDR	Climate Data Record
CMUG	Climate Modelling User Group (of ESA's CCI)
COD	Cloud Optical Depth
CRG	Climate Research Group
D/B	Data base
DOAS	Differential Optical Absorption Spectroscopy
DPM	Detailed Processing Model
EC	European Commission
ECA	ECV Core Algorithm
ECMWF	European Centre for Medium Range Weather Forecasting
ECV	Essential Climate Variable
EO	Earth Observation
ESA	European Space Agency
ESM	Earth System Model
FCDR	Fundamental Climate Data Record
FOCAL	Fast atmOspheric traCe gAs retrievaL
FP	Full Physics
FTIR	Fourier Transform InfraRed
FTS	Fourier Transform Spectrometer

GCOS	Global Climate Observing System
GEO	Group on Earth Observation
GEOSS	Global Earth Observation System of Systems
GHG	GreenHouse Gas
GMES	Global Monitoring for Environment and Security
GOSAT	Greenhouse Gas Observing Satellite
IDL	Interactive Data Language
ITT	Invitation To Tender
IODD	Input Output Data Definition
IPCC	International Panel in Climate Change
IPR	Intellectual Property Right
IUP	Institute of Environmental Physics (IUP) of the University of Bremen, Germany
JCGM	Joint Committee for Guides in Metrology
LMD	Laboratoire de Météorologie Dynamique
LUT	Look-up table
MACC	Monitoring Atmospheric Composition and Climate, EU GMES project
MERIS	Medium Resolution Imaging Spectrometer
MIPAS	Michelson Interferometer for Passive Atmospheric Sounding
MODIS	Moderate Resolution Imaging Spectrometer
N/A	Not applicable
NDACC	Network for the Detection of Atmospheric Composition Change
NASA	National Aeronautics and Space Administration
NIES	National Institute for Environmental Studies
NOAA	National Oceanic and Atmospheric Administration
OCO	Orbiting Carbon Observatory
OD	Optical Depth
OE	Optimal Estimation
PBL	Planetary Boundary Layer

PMD	Polarization Measurement Device
PR	Proxy (retrieval method)
PVP	Product Validation Plan
PVR	Product Validation Report
RA	Relative Accuracy
RD	Reference Document
RMS	Root-Mean-Square
RTM	Radiative transfer model
S5P	Sentinel-5 Precursor
SoW	Statement of work
SQWG	SCIAMACHY Quality Working Group
SRA	Seasonal Relative Accuracy
SRD	Software Requirements Document
SRON	Netherlands Institute for Space Research
SUM	Software User Manual
SVR	Software Verification Report
TANSAT	CarbonSat
TANSO	Thermal And Near infrared Sensor for carbon Observation
TBC	To be confirmed
TCCON	Total Carbon Column Observing Network
TBD	To be defined / to be determined
TROPOMI	TROPOspheric Monitoring instrument
WFM-DOAS (or WFMD)	Weighting Function Modified DOAS
WG	Working Group

***** End of Document *****